

Lew W. Myers  
Chief Operating Officer419-321-7599  
Fax: 419-321-7582

Docket Number 50-346

License Number NPF-3

Serial Number 1-1289

September 23, 2002

Mr. J. E. Dyer, Administrator  
United States Nuclear Regulatory Commission  
Region III  
801 Warrenville Road  
Lisle, IL 60532-4351

Subject: Confirmatory Action Letter Response – Revision 1 to Root Cause Analysis  
Report Regarding Reactor Pressure Vessel Head Degradation

Ladies and Gentlemen:

On April 18, 2002, the FirstEnergy Nuclear Operating Company submitted the Root Cause Analysis Report regarding the Reactor Pressure Vessel (RPV) head degradation at the Davis-Besse Nuclear Power Station, Unit 1 (DBNPS) pursuant to the Nuclear Regulatory Commission's (NRC) March 13, 2002, Confirmatory Action Letter (CAL). In concert with the Root Cause Analysis Report, which evaluated the technical issues of the RPV head condition, a Root Cause Analysis Report on Failure to Identify RPV Head Degradation was prepared to address the non-technical aspects of the condition. The non-technical Root Cause Analysis Report was submitted to NRC by FENOC letter Serial Number 1-1286, dated August 21, 2002.

The technical Root Cause Analysis Report regarding the RPV head degradation also preliminarily addressed several non-technical issues that have been more fully investigated and documented in the non-technical Root Cause Analysis Report. Therefore, the technical Root Cause Analysis Report has been revised to delete those conclusions that are more completely addressed in the non-technical Root Cause Analysis Report. The revised technical Root Cause Analysis Report regarding the RPV head degradation is enclosed. The revisions are discussed in summary in the "Purpose and Scope of the Root Cause Analysis Report" section of the enclosure.

Please be advised that this revised technical Root Cause Analysis Report does not address findings of inspections of the degraded RPV head section at Framatome ANP's facilities that have been recently reported; i.e., discovery of a previously unidentified

SEP 26 2002

Docket Number 50-346  
License Number NPF-3  
Serial Number 1-1289  
Page 2 of 2

circumferential crack in Nozzle 3 and discovery of previously unidentified cracks in the cladding area. Evaluation of these issues is continuing. It is not anticipated that the evaluations will have any effect on the conclusions of the enclosed technical Root Cause Analysis Report; therefore, no further revision of the technical Root Cause Analysis Report is contemplated.

If you have any questions or require additional information, please contact Mr. Patrick J. McCloskey, Manager – Regulatory Affairs, at (419) 321-8450.

Very truly yours,



RMC/s

Enclosure and Attachment

cc: USNRC Document Control Desk  
J.B. Hopkins, DB-1 NRC/NRR Senior Project Manager  
S.P. Sands, DB-1 NRC/NRR Backup Project Manager  
C.S. Thomas, DB-1 Senior Resident Inspector  
Utility Radiological Safety Board

Docket Number 50-346  
License Number NPF-3  
Serial Number 1-1289  
Enclosure  
Page 1 of 1

Root Cause Analysis Report

(182 Pages Follow)

Docket Number 50-346  
License Number NPF-3  
Serial Number 1-1289  
Attachment  
Page 1 of 1

**COMMITMENT LIST**

The following list identifies those actions committed to by the Davis-Besse Nuclear Power Station (DBNPS) in this document. Any other actions discussed in the submittal represent intended or planned actions the DBNPS. They are described only for information and are not regulatory commitments. Please notify the Manager - Regulatory Affairs (419-321-8450) at the DBNPS of any questions regarding this document or associated regulatory commitments.

**COMMITMENTS**

**DUE DATE**

None

---

# Root Cause Analysis Report

Significant Degradation of the Reactor  
Pressure Vessel Head

CR 2002-0891, Dated 3-8-2002

REVISION 1, DATE: 8-27-2002


Prepared by:  
S. A. Loehlein

  
Root Cause Team Lead

Reviewed by:  
J. J. Powers

  
Director

Approved by:  
L. W. Myers

  
Chief Operating Officer

## **PURPOSE AND SCOPE OF THE ROOT CAUSE ANALYSIS REPORT**

### **Purpose**

Determine the root and contributing causes for Reactor Pressure Vessel closure head (RPV head) damage experienced at nozzle 3 and minor corrosion at nozzle 2, to support the operability determination for the station's as-found condition and the future repair plan.

### **Scope**

Very early in the development of the response to this condition, it became clear that the technical causes behind the cracking of the Control Rod Drive Mechanism (CRDM) nozzles and the ensuing corrosion of the head material would draw much attention and comparison to the previously developed body of knowledge on related topics and conditions. In fact, the possibility of nozzle cracks existing at Davis-Besse was well recognized prior to the condition, but the identified significant damage to the RPV head had not been anticipated.

The unexpected finding of the significant damage at Davis-Besse immediately became a concern, both for the possible extent of condition implications at Davis-Besse and the potential impact to the industry. Therefore, the objective of the Initial Investigative Team was a prompt investigation into the primary cause(s) of the damage. The findings within this report are expected to invite input from industry experts and scientists resulting in additional study of the evidence, and further research into the topics of CRDM nozzle cracking and boric acid corrosion.

In order to provide timely insight for the plant and the industry, and to comply with the NRC's Confirmatory Action Letter on the head degradation, revision 0 of this report was prepared with the full knowledge that a number of confirmatory activities were still continuing. Revision 1 of this report is being issued as an update of the relevant technical issues associated with the RPV head damage. No changes of note have occurred in any technical conclusions from revision 0. No additional future revisions of this report are anticipated.

Management issues identified in revision 0 have been largely removed from this report, having been separately investigated in detail. The results of the management and human performance investigation appear in the Root Cause Analysis Report entitled "Failure to Identify Significant Degradation of the Reactor Pressure Vessel Head", dated 8-13-2002.

### **Investigative Team Membership**

Steve Loehlein, FENOC (Beaver Valley), Team Lead  
Chuck Ackerman, FENOC (Davis-Besse)  
Ted Lang, FENOC (Davis-Besse)  
Todd Pleune, FENOC (Davis-Besse)  
Neil Morrison, FENOC (Beaver Valley)  
William Mugge, FENOC (Davis-Besse)  
Joseph Rogers, FENOC (Davis-Besse)

### **Technical expertise provided by:**

Dr. Mark Bridavsky, FirstEnergy, Beta Labs - Failure Analysis Expert  
Stephen Hunt, Dominion Engineering – Corrosion Expert  
Steve Fyfitch, Framatome ANP, Metallurgical Expert  
Christine King, EPRI, Material Reliability Program Manager

Assessment of management aspects/decision making:

John B. Martin, Corporate Nuclear Review Board

E. J. Galbraith, Senior Representative, Assistance, Institute of Nuclear Power Operations

|

# Table of Contents

---

<u>Title</u>	<u>Page No.</u>
<b>1.0 Problem Statement</b>	1
1.1 Reason for Investigation	1
1.2 Consequences of Event/Condition Investigated	1
1.3 Immediate Actions Taken	1
<b>2.0 Event Narrative</b>	2
2.1 Background	2
2.2 Sequence of Events	3
<b>3.0 Data Analysis</b>	4
3.1 Non-Destructive Examinations of RPV Head and Nozzles	4
3.1.1 <i>Potential Evidentiary Request List</i>	5
3.1.2 <i>Locations of Cracks and Corrosion on RPV Head</i>	5
3.1.3 <i>NDE Examinations of CRDM Nozzles</i>	5
3.1.4 <i>Visual Examinations of RPV Top Head and Penetrations</i>	7
3.1.5 <i>Boric Acid Sample Results</i>	7
3.2 Cracks, Leaks and Corrosion	10
3.2.1 <i>CRDM Nozzle Cracks and Propagation to Leakage</i>	10
3.2.2 <i>Leakage Rate From CRDM Nozzle Cracks</i>	18
3.2.3 <i>Source of Boric Acid Deposits on RPV Head</i>	22
3.2.4 <i>Corrosion of RPV Top Head Surface</i>	23
3.3 Investigation of Lead Indicators	29
3.3.1 <i>Timeline</i>	29
3.3.2 <i>Sequence of Relevant Events</i>	30
3.3.3 <i>CRDM Flange and RPV Head Inspections during Refueling Outages</i>	30
3.3.4 <i>Containment Air Cooler Cleaning</i>	35
3.3.5 <i>Containment Radiation Monitor RE4597 Observations &amp; Filter Plugging</i>	37
3.3.6 <i>Containment Recirculation Fan/Fan Failures</i>	40
3.4 Programs Important to Preventing Problems	41
3.4.1 <i>B&amp;W Owners Group and Industry CRDM Nozzle Related Initiatives</i>	41
3.4.2 <i>Davis-Besse Boric Acid Corrosion Control Program</i>	46
3.4.3 <i>Davis-Besse Inservice Inspection Program</i>	48
3.4.4 <i>Evaluation of Condition Report Responses</i>	49
3.5 Related Issues	50
3.5.1 <i>RPV Head Inspections</i>	50
3.5.2 <i>Restart Readiness</i>	51
3.6 Causal Factors/Conclusions	51



<b>4.0 Experience Review</b>	54
4.1 Davis-Besse Experience	54
4.2 Nuclear Industry Experience	54
4.3 Conclusions	54
<b>5.0 Root Cause Determination</b>	55
5.1 Probable/Root Causes	55
5.2 Contributing Causes	55
<b>6.0 Extent of Condition</b>	56
6.1 Degradation Mechanism Issues	56
<b>7.0 Recommended Corrective Actions</b>	58
7.1 Probable/Root Causes Corrective Actions	58
7.2 Contributing Causes Corrective Actions	59
7.3 Additional Actions	59
<b>8.0 References</b>	61
8.1 Davis-Besse References	61
8.2 Vendor References	63
8.3 NRC References	64
8.4 INPO References	65
8.5 Industry References	66
8.6 Other References	66
<b>9.0 Personnel Interviews</b>	67
9.1 Personnel Interviewed	67
9.2 Personnel Consulted	68
<b>10.0 Methodologies Employed</b>	69

# Tables

---

<u>Title</u>	<u>Page No.</u>
1. Nozzle 1 NDE Examination Results	70
2. Nozzle 2 NDE Examination Results	71
3. Nozzle 3 NDE Examination Results	72
4. Nozzle 5 NDE Examination Results	73
5. Nozzle 47 NDE Examination Results	74
6. Comparison of Davis-Besse to Other B&W Design Plants	75
7. Nuclear Industry Experience Review Results	76

# Figures

<u>Title</u>	<u>Page No.</u>
1. Davis-Besse RPV Top of Head Section View	88
2. Davis-Besse RPV Top of Head Plan View	89
3. Davis-Besse CRDM Nozzle General Arrangement	90
4. Boric Acid and Iron Oxide on Vessel Flange at 12RFO	91
5. Nozzle 2 Corrosion Area Location, Size, and Profile	92
6. Cavity in Reactor Vessel Head between Nozzle 3 and 11	93
7. Locations of Cracks and Corrosion on Davis-Besse RPV Head at 13RFO	94
8. Nozzle 1 Crack Locations and Sizing	95
9. Nozzle 2 Crack Locations and Sizing	96
10. Nozzle 3 Crack Locations and Sizing	97
11. Nozzle 5 Crack Locations and Sizing	98
12. Nozzle 47 Crack Locations and Sizing	99
13. Corrosion and Possible Impingement at Nozzle N-3	100
14. Nozzle 3 Clad Thickness Measurements	101
15. Hoop Stresses and Operating Condition Deflections in CRDM Nozzles 2-5	102
16. Location of Leaking Nozzles in B&W Design Plants	103
17. Distribution of Leaking Nozzles in B&W Design Plant	104
18. CRDM Nozzle Leakage Observed at Oconee 3	105
19. Unidentified Leak Rate at Davis-Besse (Cycle 13)	106
20. As Found Locations of Boric Acid Deposits on Davis-Besse Vessel Head (10RFO to 13RFO)	107
21. Nozzle Crack Leakage Rate Calculation Results	108
22. Finite Element Model Boundary Conditions to Simulate Axial Crack	109
23. Crack Opening Displacement with the Crack Surface Nodes Released	110
24. Boric Acid Deposits on Top of Head at Start of 13 RFO	111
25. Corrosion Rate for EPRI Experiments (Proprietary)	112
26. Timeline of Key Events Related to Reactor Vessel Head Boric Acid Wastage	113
27. Events & Casual Factor Chart	114a-e

<u>Title</u>	<u>Page No.</u>
28. Leaking Flanges Found and Repaired During Each Outage	115
29. Flange Leakage with Stalactite Formation from Insulation and Stalagmite Formation on top of Reactor Vessel Head (8RFO)	116
30. Flange Leakage Crusted On Side of Nozzles and Stalactites from Gaps in Insulation (8RFO)	117
31. Reddish Brown Boron Deposits Crusted on Side of Nozzle (8RFO)	118
32. Boron Deposits – Source Unclear (8RFO)	119
33. North Side of Reactor Vessel Head (10RFO)	120
34. Boron Deposits Near Top of Reactor Vessel Head (10RFO)	121
35. Typical Deposits for Periphery (10RFO)	122
36. Red Rusty Boric Acid Deposits on Vessel Flange (12RFO)	123
37. Boron Piled Under the Insulation (11RFO)	124
38. Boric Acid Deposits with Heavy Iron Concentration on Underside of Nozzle 3 (13RFO)	125
39. 2000 Interferences with CRDM Flange Inspection	126
40. RE4597 Sample Location	127
41. CTMT Radiation Monitors RE4597AA/BA (Combined Iodine Channels)	128
42. CTMT Radiation Monitors RE4597AA & BA (Both Noble Gas Channels)	129
43. Potential Effects of Boric Acid Deposits on Vessel Top Head Surface	130
44. Crack Profile for Nozzle 3, Flaw #1	131

# Attachments

---

<u>Title</u>	<u>Page No.</u>
1. Potential Evidentiary Request List (Rev. 4)	132
2. Sequence of Relevant Events	135

# 1.0 Problem Statement

---

## 1.1 Reason for Investigation

Significant degradation of the reactor pressure vessel top head base metal was discovered at nozzle 3 (toward nozzle 11) and minor corrosion at nozzle 2 during the thirteenth refueling outage (13RFO) in March, 2002.

This root cause report addresses the cause of the loss of RPV head base metal in the region of nozzles 3 and 2.

## 1.2 Consequences of Event/Condition Investigated

The RPV head is an integral part of the reactor coolant pressure boundary, and its integrity is vital to the safe operation of the plant. Degradation of the RPV head or other portions of the reactor coolant pressure boundary can pose a significant safety risk if permitted to progress to the point where there is risk of a loss of coolant accident. Analysis indicates that the as-found condition of the affected nozzles would not have been expected to result in failure of the pressure integrity of the reactor coolant system. However, the degraded condition had been progressing over a period of time, without knowledge of the condition.

## 1.3 Immediate Actions Taken

1. At the time of discovery, the plant was already in a safe, shutdown condition. Ongoing outage activities related to the repair of the CRDM nozzle on the RPV head were suspended.
2. A root cause evaluation team was convened to perform the initial investigation.
3. A plan was created to preserve and collect, evidence necessary for the investigation.

# 2.0 Event Narrative

## 2.1 Background

Davis-Besse is a raised loop pressurized water reactor (PWR) manufactured by Babcock and Wilcox (B&W). The reactor licensed thermal power output is 2772 megawatts. The plant achieved initial criticality on August 12, 1977. The RPV has an operating pressure of 2155 psig and a design pressure of 2500 psig. Davis-Besse has accumulated 15.78 effective full power years (EFPY) of operation when the plant was shut down for 13RFO.

The RPV head has 69 CRDM nozzles welded to the RPV head of which 61 are used for CRDMs, seven are spare, and one is used for the RPV head vent piping. Each CRDM nozzle is constructed of Alloy 600 and is attached to the RPV head by an Alloy 182 J-groove weld. The RPV head is constructed of low-alloy steel and is internally clad with stainless steel. Figures 1, 2 and 3 show the arrangement of the Davis-Besse RPV head. Figure 1 is a section view through the RPV centerline, Figure 2 is a plan view from the top of the RPV closure head, and Figure 3 shows how the CRDM nozzles are welded into the RPV head.

Throughout this report the CRDM nozzles will be addressed as nozzles 1, 2, ...69 and not the associated nozzle core grid location. Given that many of the sources referenced during the root cause analysis utilized the nozzle core grid location, the list below provides a correlation between the CRDM nozzle and core grid location.

<u>CRDM NOZZLE #</u>	<u>CORE GRID LOCATION</u>	<u>CRDM NOZZLE #</u>	<u>CORE GRID LOCATION</u>	<u>CRDM NOZZLE #</u>	<u>CORE GRID LOCATION</u>
1	H8	24	N8	47	D12
2	G7	25	H4	48	N12
3	G9	26	E5	49	N4
4	K9	27	E11	50	C5
5	K7	28	M11	51	C11
6	F8	29	M5	52	E13
7	H10	30	D6	53	M13
8	L8	31	D10	54	O11
9	H6	32	F12	55	O5
10	F6	33	L12	56	M3
11	F10	34	N10	57	E3
12	L10	35	N6	58	B8
13	L6	36	L4	59	H14
14	E7**	37	F4	60	P8
15	E9*	38	C7	61	H2
16	G11*	39	C9	62	B6
17	K11*	40	G13	63	B10
18	H9*	41	K13	64	F14
19	M7*	42	O9	65	L14
20	K5*	43	O7	66	P10
21	G5*	44	K3	67	P6
22	D8	45	G3	68	L2
23	H12	46	D4	69	F2

\*Spare nozzles

\*\*Head vent connection

On August 12, 2001, Davis-Besse received Nuclear Regulatory Commission (NRC) Bulletin 2001-01 Circumferential Cracking of Reactor Pressure Vessel Head Penetration Nozzles (reference 8.3.5). In discussion held with the NRC on November 28, 2001, in response to this bulletin, Davis-Besse committed to a 100% qualified visual inspection, non-destructive examination (NDE) of 100% of the CRDM nozzles and characterization of flaws through destructive examination should cracks be detected. During performance of these inspections during 13RFO significant degradation of the RPV top head base metal was discovered between nozzles 3 and 11 and some minor corrosion at nozzle 2 in March 2002.

## 2.2 Sequence of Events

Because the sequence of events is in part developed based upon inferred information rather than conclusive validated facts, a sequence of events will not be discussed here. Instead the data analysis section will develop the bases for the sequence of events in determining the associated causes. Attachment 2 provides a sequence of relevant events from source documents reviewed during the root cause analysis process. Figures 26 and 27 provide a timeline of key events related to RPV head boric acid corrosion and the event and causal factors chart that provide a summary level sequence of events information developed as a result of the data analysis.



# 3.0 Data Analysis

---

The data analysis section provides a summary of the data gathered during the root cause investigation. The data gathered for this analysis is from related potential condition adverse to quality reports (PCAQRs) and condition reports (CRs), the System Engineer's System Performance Book, pictures taken during inspections, personnel interviews, procedures, and other documents identified in the references section.

## 3.1 Non-Destructive Examination of RPV Head and Nozzles

The following is a summary of the non-destructive examination effort on the cracked nozzles and degraded RPV head. After removal of insulation from the RPV flange early in 13RFO, boric acid crystal deposits and iron oxide were found to have flowed out from several of the openings (mouse holes) in the lower service structure support skirt (Figure 20). Figure 4 shows deposits on the flange during the inspection in the twelfth refueling outage (12RFO).

Blade probe ultrasonic (UT) examination of the CRDM nozzles from below the RPV head for circumferential cracks and large axial cracks, identified axial cracks in nozzles 1, 2, 3, 5, 47, and 58. Supplemental top-down UT examination of these nozzles confirmed through-wall axial cracks extending above the J-groove weld elevation in nozzles 1, 2 and 3. Axial cracks were confirmed in nozzles 5 and 47, but they did not extend above the top of the J-groove weld and would not have caused a leak. Axial cracking was not confirmed in nozzle 58. A small (34° arc length and 0.34" deep) circumferential crack was discovered above the J-groove weld on the outside of nozzle 2 on the downhill side. It was determined that all five nozzles would be repaired by boring out the lower part of the nozzle containing the cracks, and rewelding the end of the nozzle to the opening in the RPV head using the Framatome ANP repair method.

After removing the lower part of nozzle 3, a cavity was discovered in the low-alloy steel RPV head material above the J-groove weld on the downhill side. Additionally, after removing the lower part of nozzle 2, a smaller area of corrosion of the low-alloy steel RPV head material was discovered between the bottom of the machined nozzle and the top of the J-groove weld (Figure 5). This area of corrosion was found to extend under the portion of the nozzle left in place after machining.

After pulling nozzle 3 and cleaning by hydrolasing, the top of the RPV head was inspected using a video camera on a long pole through the vacated nozzle 3 penetration. This inspection showed a large cavity in the low-alloy steel RPV head material between nozzles 3 and 11 (Figure 6). The area with missing material was reported as being about 6.6" long and approximately 4-5" at the widest point. Ultrasonic thickness measurements from the underside of the RPV head showed the thickness of the remaining material (cladding) to be an average of approximately 0.3", which is greater than the 3/16" nominal or 1/8" minimum specified clad thickness. The videotape inspections also showed a small area of corrosion where nozzle 2 penetrates the RPV top head surface. The small area of corrosion at the top of nozzle 2 was found to lie directly over the area of corrosion at the bottom of nozzle 2 as seen in Figure 5. The videotape inspection also showed evidence of a small leak path where nozzle 1 penetrates the RPV top head surface.

### 3.1.1 Potential Evidentiary Request List

One of the first priorities of the root cause evaluation team was to collect and preserve the evidence necessary to facilitate the root cause evaluation. A Potential Evidentiary Request List was created specifying the evidence to be collected and preserved and the reason for collecting the evidence. The list was revised several times throughout the evaluation (see Attachment 1, which is current to early April, 2002). This list was used to create integrated examination and inspection plans for field implementation.

### 3.1.2 Locations of Cracks and Corrosion on RPV Head

Figure 7 shows locations of cracks and corrosion on the Davis-Besse RPV top head surface. This figure is included to serve as a reference for the following descriptions of the degraded areas.

### 3.1.3 NDE Examinations of CRDM Nozzles

Automated ultrasonic examinations of all 69 CRDM nozzles were performed from beneath the RPV head using the ARAMIS inspection tool and a "Circ." blade probe. The techniques utilized for this examination are intended for the detection and through-wall (depth) sizing of circumferential inside diameter (ID) and outside diameter (OD) initiating flaws in the nozzle base metal only. Forward scatter time of flight detector (TOFD), longitudinal-wave techniques are used. The examinations were conducted from the bore of the CRDM nozzles in the J-groove weld region of the nozzle.

The examinations performed with the blade probe consisted of scanning for circumferential and significant axial flaws within the nozzle wall. The tooling consisted of a blade containing a nominal 5 MHz, 50 degree TOFD transducer set. The circ. blade probe provides flaw detection (axial and circumferential flaws) and sizing (non-axial flaws) information. For the forward scatter transducers, flaw detection is identified by loss of signal response either from the lateral wave or backwall responses as well as the presence of crack tip diffracted responses.

Prior to the examinations, demonstrations were performed using the Electric Power Research Institute (EPRI)/Materials Reliability Program (MRP) samples removed from Oconee. This demonstration showed that circumferential and axial flaws can be detected with the circ. blade probe.

During the initial examination, some nozzles had areas where the gap between the nozzle and the leadscrew mechanism was too narrow to insert the probe. All of these areas were rescanned after the initial inspection by moving the leadscrew support tube to open the gap for examination.

The examination with the blade probe identified potential flaw indications in nozzles 1, 2, 3, 5, 47 and 58. Because almost all of the flaws detected on these nozzles were characterized as axial, only limited information was available with the circ. blade probe. These axial flaws could have been characterized using axial blade probes. However, because there was a high probability that these nozzles would require repair, the CRDMs for these nozzles were removed to perform additional UT examination using the top-down tool.

The top-down tool contains 10 transducers and provides the ability to detect and characterize axial and circumferential flaws and also provides additional information required for the repair activity. Images of the nozzles identified for repair are included in the reference 8.1.1 report and show the various features required to implement the repair. These generally include the location of the RPV head OD, the elevation of the proposed cut line, and the location of the top of the J-groove weld.

Automated ultrasonic examinations of CRDM nozzles 1, 2, 3, 5, 47 and 58 were performed using the top-down inspection tool. The techniques utilized for the examination are intended for the detection and through-wall (depth) sizing of axial and circumferential ID and OD initiating flaws in the nozzle base metal only. Forward scatter, longitudinal-wave and backward scatter shear wave techniques were used. The examinations were conducted from the bore of the CRDM nozzles in the J-groove weld region. The potential flaw indication on nozzle 58 was determined to be a false indication using the top-down tool, potentially due to nozzle ovality.

The inspections consisted of scanning for axial and circumferential flaws within the nozzle. The tooling consisted of a transducer head that holds 10 individual search units. These search units were divided into two sets, one for the axial beam direction and one for the circumferential beam direction. The axial beam search units consisted of 5.0 MHz, longitudinal wave forward scatter time of flight search units with angles of 30° and 45°; backward scatter pulse echo, 2.25 MHz 60° shear wave search units; and a 5.0 MHz 0° search unit. The circumferential beam search units consisted of 5.0 MHz, longitudinal wave forward scatter time of flight search units with angles of 45°, 55°, and 65°; backward scatter pulse echo, 2.25 MHz 60° shear wave search units; and a 5.0 MHz 0° search unit.

The detection of flaw indications is based upon the expected responses for each search unit and technique. The 0° transducer provides weld position information and also provides positional information regarding any lack of backwall response in the region of the flaw. The forward scatter time of flight techniques provide flaw detection and sizing information. For the forward scatter transducers, flaw detection is identified by loss of signal response either from the lateral wave or backwall responses as well as detection of crack tip diffracted responses. The 60° shear wave transducer provides detection by means of corner trap responses between the flaw and nozzle surface and sizing with tip diffracted signals.

Reference 8.1.1 contains the data sheets from ultrasonic examination of the six CRDM nozzles that were identified as having flaws with the blade probe. Included in this report are the data sheets for the blade UT and the rotating UT using the top-down tool. Images of the UT data are also included to show the features identifying detected flaws.

The data was also reviewed for evidence of a leak path in the penetration bore with the blade and rotating UT techniques. Leak paths were detected in nozzles 1, 2, and 3 with blade and rotating UT. Images of the leak paths are included in the reference 8.1.1 report. Subsequent review by EPRI of all UT results indicated that although nozzle 46 had no detected cracks, some evidence of a leakage flow path was identified, due to the characteristics of the backwall reflection.

The examination results are summarized in the following table:

Nozzle #	Summary of NDE Results
1	9 Axial Flaws, 2 through-wall (TW) with a leak path
2	9 Axial Flaws, 1 Circ. Flaw, 6 TW with a leak path
3	4 Axial Flaws, 2 TW with a leak path
5	1 Axial Flaw
46	No Flaw Indication, potential leak path
47	1 Axial Flaw
58	No Recordable Indications

A pictorial layout of the identified flaws in nozzles 1, 2, 3, 5 and 47 is provided in Figures 7-12. Detailed NDE results are provided in Tables 1-5.

### **3.1.4 Visual Examinations of RPV Top Head and Penetrations**

Visual examinations were made of the RPV top head surface both before and after removing a section of insulation over the nozzles of concern. The RPV head penetrations were also examined following removal of nozzles 2 and 3. Results of these examinations were as follows:

#### **Degradation at Nozzle 3**

Degradation observed at nozzle 3 is pictorially shown in Figure 13. The 180° (uphill toward nozzle 1) location is essentially intact, with little to no degradation. The 0° (downhill toward nozzle 1) location exhibits the worst degradation, with the low-alloy steel material corroded away, down to the stainless steel cladding, for approximately 6.6 inches in length and 4 to 5 inches at the widest part. Figure 14 shows cladding thickness measurements made by UT from the underside of the RPV head. (Note: There are several low readings outside the designated area of damage. These are attributed to inclusions or bad readings. These readings do not correspond with visual observations, and will be further verified following excavation of the damaged area.)

From the 270° location to the 0° location (counterclockwise looking down from the top of the RPV head), there is a large undercut area. From the 0° location to the 90° location (counterclockwise looking down from the top of the RPV head), the corrosion is less.

#### **Degradation at Nozzle 2**

Degradation was observed at nozzle 2 following the initiation of repair efforts. Figure 5 shows the observed area of corrosion. The overall corroded area, based on the video examination and approximate measurements from the impression, is 3-1/2 to 4 inches in length starting from the top of the RPV head, about 3/8 inch deep (at the deepest location approximately 1-3/4 inches from the top of the RPV head), and between 1-1/4 to 2 inches at its widest location. The depth of corrosion decreased as the annulus opening was approached. This type of corrosion profile is similar to testing that has been performed by EPRI (reference 8.5.3) regarding location of the deepest corrosion and the fact that it could have been identified on the top of the RPV head.

#### **Degradation at Nozzle 1**

The observed degradation at the nozzle 1 location is minimal. A small, crevice (<1/16 inch wide and about 3/4 inch circumferentially), located at the 270° location (looking down from top of RPV head clockwise with 0° in the West direction), was identified at the surface of the RPV head. The observed degradation at nozzle 1 was within the boundary of the pre-established repair plan.

### **3.1.5 Boric Acid Sample results**

Boric Acid Samples were taken from the reactor head prior to cleaning as well as from nozzle 3 and from the nozzle 2 cavity. These sample results are reported in reference 8.2.14 and 8.2.15. As with all sample collection, the purity of the sample and the accuracy of its collection are critical. The samples taken from the reactor head were collected by scooping the material with a long handled tool. Due to the difficulty of collecting the field samples, the probability of cross contamination is fairly high and could lead to false or compromised results. In addition, transport of boric acid and corrosion products in aerosol or liquid form almost certainly caused some mixing of old deposits with newer deposits. However, a selection of the sample results as

determined by inductively coupled plasma mass spectroscopy (ICP-MS)) is reproduced in the following table from reference 8.2.14:

<u>Element</u>	<u>Location of sample:</u>				
	<u>N2-N1</u>	<u>N1-N3</u>	<u>N7</u>	<u>N2</u>	<u>N3 flange</u>
Boron (ppm)	163000	86300	99500	130000	61700
Iron (ppm)	100000	269000	157000	220000	359000
Lithium (ppm)	17000	10800	9900	13000	11300
Chrome (ppm)	7790	54100	7100	3900	5800
Nickle (ppm)	3120	6000	1600	2100	1800
B/Li ratio	9.6	8.0	10.1	10.0	5.5
Fe/B ratio	0.61	<b>3.12</b>	1.58	1.69	<b>5.82</b>
Cr/B ratio	0.048	<b>0.63</b>	0.071	0.030	<b>0.094</b>
Ni/B ratio	0.019	<b>0.070</b>	0.016	0.016	<b>0.029</b>
Cr/Ni ratio	2.49	<b>9.01</b>	4.43	1.85	3.22
Cs 134/137	0.14	1.11	0.61	0.41	NA
Age (date)	6/1999	<b>8/2001</b>	10/2000	3/2000	NA

The entries titled N2 –N1 and N1-N3 signify that the sample was collected between those nozzles. The most compelling conclusion that can be taken from the above data is that the age of the sample in the proximity of nozzle 3 was the most recent. This supports that the material originated predominantly from nozzle 3.

The nozzle 3 area sample (N1-N3) also had a considerably higher iron content than the rest of the material collected from the reactor head. Additionally, the chromium/boron ratio and the chromium to nickel ratio are relatively high. This could be evidence that this recent material had been in more intimate contact with the 309 Stainless Steel cladding material than the other samples. 309 Stainless Steel has a higher chromium content than the nickel-based alloy 600 nozzle material. Therefore, some evidence is provided that the earlier samples did not effectively contact the liner, i.e. that the corrosion proceeded predominantly from the top of head downward. As the corrosion front reached the liner, the most recent deposits acquired more chromium.

Boron to Lithium ratios indicate that leakage occurred during startup or power operation when significant Lithium is present. However, the boron to lithium ratio is much lower than reactor coolant, perhaps indicating that volatile loss of lithium is different from that of boron.

The age of deposits from the bottom of the N3 flange may support that the material was ejected upward to this location at an earlier time, when corrosion of iron was proceeding, but the liner had not yet been reached. The underlying assumption is that the annulus was significantly narrower when the nozzle 3 flange acquired the deposits. A narrow, intact annulus would produce a focused upward jet of leakage and entrained corrosion products to deposit on the bottom of the nozzle 3 flange. By the time that the stainless steel cladding was reached, the annulus would have been consumed by the corrosion front. At that point, the upward velocity

would be reduced, despite a potentially greater leak rate. Cesium dating of the nozzle flange deposits could either dispel or help to confirm this theory. However, confirmation of this effect is beyond the necessary scope of this report. The EPRI MRP may clarify this point through continuing corrosion modeling efforts.

References 8.2.15 and 8.2.14 (respectively) also provide X-ray diffraction analysis of the chemical compounds found in the samples of nozzle 2 corrosion products (removed after head cleaning) and of the samples boric acid on the head discussed above. Essentially, the principle compounds found were Iron Borate ( $\text{Fe}_3\text{BO}_6$ ), Maghemite (or "red rust" -  $\text{Fe}_2\text{O}_3$ ), Sassolite (or Boric Acid -  $\text{H}_3\text{BO}_3$ ), Goethite ( $\text{FeOOH}$ ), and Metaborite ( $\text{HBO}_2$ ). Traces (<5wt%) of Iron Carbide and Lithium compounds were also noted at some locations. The nozzle 1 area, very near nozzle 3, was highest in Maghemite. The nozzle 3 area was mostly Iron Borate, with some Sassolite and Metaborite. This was similar to the deposits under the flange of nozzle 3, which were nearly exclusively Iron Borate. This provides additional evidence that the deposits under the nozzle 3 flange originated from the nozzle 3 cracks. Interestingly, Sassolite was found at greater than 25 weight percent only in the nozzle 2 and 7 area samples.

Inside the nozzle 2 cavity (it should be noted that these samples would have been taken after head cleaning with water), major constituents (> 25wt%) were Magnetite ( $\text{Fe}_3\text{O}_4$ ) and Hematite ( $\text{Fe}_2\text{O}_3$ ). Medium constituents (10-25wt%) were Maghemite, Iron Borate, and Lithium Iron Oxide. Minor and Trace constituents included Nickel and Chromium compounds. The presence of the black iron oxide inside the cavity, Magnetite, may be noteworthy. This compound tends to form in a restricted oxygen environment and was not noted in the samples on top of the head. Conversely, Maghemite ( $\text{Fe}_2\text{O}_3$ ) was found at high levels at selected locations both on top of the head and inside the nozzle 2 cavity.

In summary, although sample integrity is not assured, the sample results are consistent with other evidence that the material on the reactor head originated primarily at nozzle 3, and flowed or extruded away from that location. This is supported both by the aging and by the elemental analysis. The material on top of the head appeared to be well oxygenated, with more restricted oxygenation in the nozzle 2 cavity.

## 3.2 Cracks, Leaks and Corrosion

This data analysis section is a technical review of the causes of cracks and leaks throughout the industry, and the resultant corrosion of the RPV top head surface. This information provides key inputs to the probable cause determination.

### 3.2.1 CRDM Nozzle Cracks and Propagation to Leakage

The following is a review of cracking experience in Alloy 600 RPV head CRDM nozzles, and identification of the possible causes of cracks in Davis-Besse nozzles 1, 2, 3, 5 and 47.

#### Primary Water Stress Corrosion Cracking of Alloy 600 and Alloy 82/182 Materials

There have been numerous incidents of cracked Alloy 600 nozzles, and Alloy 82/182 welds, in domestic non-steam generator related PWR plant primary system applications since a pressurizer instrument nozzle leak at San Onofre 3 in 1986. These applications include pressurizer instrument nozzles, pressurizer heater sleeves, hot leg piping instrument nozzles, CRDM nozzles, steam generator drain nozzles, RPV outlet nozzle butt welds, and a pressurizer spray line safe end. In all cases, the leakage has been discovered before failure of the components.

In all but a few cases, cracking in nozzle applications has been attributed to primary water stress corrosion cracking (PWSCC). The mechanism of PWSCC is not completely understood, and prediction of crack initiation time has proven to be difficult, if not impossible. It is known, however, that PWSCC of Alloy 600 occurs as a result of the following three factors:

- A susceptible material
- A high tensile stress (including both operating and residual stress) at J-groove welds, roll expansions, and expansion transitions
- An aggressive environment (PWR primary water at high temperature)

The few exceptions are related to weld defects (Ringhals J-groove welds) and resin intrusions (Zorita). These incidents are documented in EPRI TR-103696, PWSCC of Alloy 600 Materials in PWR Primary System Penetrations (reference 8.5.4).

The susceptibility of Alloy 600 material depends on several factors including the chemical composition, heat treatment during metal production, heat treatment during fabrication of the component, and operating parameters. Alloy 600 is known to be susceptible to PWSCC with some heats of material being more susceptible than others principally due to a poorer microstructure.

High stresses are induced into the nozzle by the J-groove weld. Since the RPV head is stiff relative to the nozzle wall, shrinkage of the J-groove weld during cooling pulls the nozzle wall radially outward causing high tensile hoop stresses as shown in Figure 15 (the deflections in Figure 15 are exaggerated to illustrate the welding induced distortion). If the nozzle is machined prior to welding, higher stresses can be induced in the cold worked machined surface.

Questions arose from readers of revision 0 of this report asking if PWSCC cracks could initiate due to welding or fabrication stresses at conditions of reduced temperature and pressure. PWSCC has been the subject of much research and analysis in recent years as a result of the many leaks that have been attributed to PWSCC. It is generally accepted that the initiation time for a given crack can be estimated by a standard Arrhenius activation energy approach. For example, in reference 8.5.11, a temperature adjusted degradation time was developed to rank plant susceptibility as compared to a reference temperature. The equation presented (simplified for a single operating temperature) is

$$EDY_{600F} = \Delta EFPY \exp [-Q_i/R(1/T_{head}-1/T_{ref})]$$

Where:

$EDY_{600F}$	= Effective Degradation Years, normalized to 600°F
$\Delta EFPY$	= Effective Full Power Years
$Q_i$	= Activation Energy for Crack initiation (50 kcal/mol)
$R$	= universal gas constant ( $1.103 \times 10^{-3}$ kcal/mol-°R)
$T_{head}$	= Full power head temperature (°R)
$T_{ref}$	= Arbitrary reference temperature (600 °F = 1059.67°R)

Using this equation, with a EFPY = 14.7 years through February 2001, and a head temperature of 605 °F, this equation placed Davis-Besse at 17.97 EDY, or 7th in calculated susceptibility as compared to all US PWRs.

As implied above, the actual initiation time of a crack is also related to both the microstructure of the alloy, and the state of stress of the component. Typically, the stresses of importance are those that are induced by fabrication (e.g. welding), which can be large compared to operational stresses. Equations have been proposed to take these factors into account. However, the parameters of interest are rarely known in the field and the sensitivity is lower than that of temperature. For time spent at less than full temperature, for example at 200 °F, the above equation indicates that the EDY accumulates at only  $5 \times 10^{-12}$  of the rate at 600°F. Therefore, the practice tends to simply utilize an equation similar to the above, and compare the predicted EDY to the EDY at onset of failures in similar components. Thus, a comprehensive and accurate crack initiation model has yet to be developed. Nonetheless, the current understanding and models in use support the conclusion that exposure to long periods at low temperature and pressure does not measurably affect the predicted crack initiation time.

#### **Effect of Alloy 600 Heat Treatments**

Chemical composition and heat treatment are interrelated in several ways. For example, one reason for annealing Alloy 600 is to solutionize the carbon in the alloy. As the material cools, the available carbon and chromium will precipitate (in the form of chromium carbides) from solution at both intragranular and intergranular locations. If the cooldown from the anneal is sufficiently slow, a greater number of carbides will precipitate at the grain boundaries (i.e., intergranularly), and the resistance to PWSCC will be improved.

Well decorated grain boundaries are an indication that an Alloy 600 material has received a proper heat treatment and that sufficient carbon was available in solution to combine with chromium. If adequate amounts of carbon and chromium exist, but the anneal was not at a high enough temperature or sufficient time was not allowed to solutionize the carbon, an adequate amount of carbon will not be available to precipitate intergranularly as chromium carbides, leading to minimal grain boundary decoration. For example, a temperature of 1850°F is necessary to solutionize material with a carbon content of 0.04%.

The actual annealing temperatures for the Davis-Besse CRDM nozzle Alloy 600 materials could not be located. However, the minimum range of annealing temperatures used by the



manufacturer (B&W Tubular Products) at the time was 1600-1700°F. Therefore, it can be assumed that the microstructure of the heats of material utilized on the Davis-Besse RPV head is likely to be less than optimum relative to resistance to PWSCC. Additional information on the microstructure will be obtained during destructive examinations of nozzles 3 and 2, but this is not expected to affect the contents of this report (see section 7.3.3).

### **RPV Head Nozzle and Weld Leakage Experience**

The first leak from an RPV head CRDM nozzle occurred at the EdF Bugey 3 plant in France in 1991. A small amount of leakage [ $<1$  liter/hr (0.004 gpm)] was discovered on the outside surface of the RPV head during a primary system hydrostatic test. Investigation showed the leak was from a through-wall crack in an outer row CRDM nozzle that had initiated from the inside surface. Failure analysis confirmed that the crack was PWSCC and that contributing factors included susceptible material microstructure, stress concentration at a counterbore on the nozzle inside surface, high hardness of the cold worked machined surface, and high residual tensile stresses induced in the nozzle during welding.

Subsequent to the Bugey 3 experience, PWSCC of Alloy 600 base metal and welds has been discovered in other PWR RPV heads worldwide. In 1994 a partial through-wall crack was found at DC Cook 2. Like the Bugey 3 crack, the crack at DC Cook 2 initiated on the ID surface of the nozzle at the elevation of the J-groove weld. CRDM nozzle inspections have also found shallow craze cracking on the nozzle ID near the weld in a few nozzles at Oconee 2 and Millstone 2.

As of February 2000, about 6.5% of all EdF nozzles inspected had been found to contain cracks and about 1.25% of inspected nozzles in other plants worldwide had been found to contain cracks greater than the minimum measurable depth of about 2 mm (0.08 inches). Further details regarding the extent of condition are provided in MRP-44, Part 2, PWR Materials Reliability Program – Interim Alloy 600 Safety Assessments for US PWR Plants, Part 2: Reactor Vessel Top Head Penetrations (reference 8.5.5).

In November 2000 a through-weld leak at a CRDM nozzle weld at Oconee 1 was attributed to PWSCC. Laboratory analysis of a boat sample removed from this weldment confirmed that the crack was PWSCC.

In February 2001, PWSCC was detected in nine nozzles at Oconee 3 that were from one material heat (M3935) that had a yield strength of 48.5 ksi. Most of these cracks were axial and initiated on the nozzle OD surface. However, some axial cracks had initiated on the ID and propagated partially through the wall. In addition, most of the cracks that were found in Oconee 3 nozzles initiated below the weld, similar to those found at Davis-Besse. However, three Oconee 3 nozzles contained OD circumferential cracks above the weld.

In April 2001, Oconee 2 performed a visual inspection of the RPV head during a refueling outage at the end-of-cycle 18 (approximately 21 EFPY). Boric acid crystals were observed at four CRDM nozzles. The inspections performed at Oconee-2 in 2001 identified OD crack-like axial indications below the weld on all four nozzles. Ultrasonic examinations showed that these indications were OD-initiated and that none of the indications were through-wall. An OD-initiated circumferential indication, 0.1 inch (2.5 mm) in depth and 1.26 inch (32 mm) in length, was noted above the weld on one of the nozzles. Eddy current examinations of the ID of the nozzles revealed shallow craze-type flaw clusters in all four nozzles that were distributed around the entire ID circumference (360° and above the weld). Based on these results, the leak path was through the interface between the nozzle and the J-groove weld.

In November 2001, a visual inspection of the top surface of the Oconee 3 reactor RPV head showed evidence of primary water leakage on the RPV head surface. This inspection was performed in accordance with Duke Energy's response to NRC Bulletin 2001-01 as a "Qualified Visual" inspection. Boric acid deposits with a wet appearance were identified around four CRDM nozzles and determined to be probable leak locations. Three additional CRDM nozzles were identified as being masked by boric acid crystal deposits from an indeterminate leakage flow path and were therefore classified as possible leaking nozzles. This is the same visual inspection performed during the previous outages except that a VT-2 qualified inspector participated. UT examinations showed that five nozzles had indications that extended from below the weld to above the weld indicating a leak path in addition to various other ID and OD indications. One nozzle had a circumferential indication in the nozzle above the weld. Seven CRDM Nozzles were repaired during this outage using the automated Framatome-ANP "ID Ambient Temper Bead Repair" technique that is being employed at Davis-Besse.

At least five other PWRs have identified similar PWSCC in the last year.

In summary, since November 2000, leaks have been discovered from at least 30 CRDM nozzles at PWRs in the United States. Most of the leaks have been through axial cracks in the nozzle base material, but some have also been through axial/radial oriented cracks in the J-groove welds. Investigation of these leaks has led to the discovery of circumferential cracks above the J-groove weld at some plants, including 165° through-wall circumferential cracks in two nozzles at Oconee 3.

None of these plants reported loss of material due to general corrosion that was similar to Davis-Besse nozzle 3.

#### **RPV Head Corrosion Associated with Boric Acid**

There have been several earlier cases of significant corrosion of low alloy steel on the reactor head. For example, in 1970, Beznau unit 1 (Switzerland) developed a canopy seal weld leak that was sufficient to cause fouling of the containment air coolers. Left in service for 2 months after being noted due to the fouling, the leak succeeded in promoting corrosion of the low alloy steel head over an area 50mm wide and 40mm deep. However, the head was analyzed and returned to service without repair. Leakage for the Beznau event was estimated at 0.02 gpm. In 1986, a conoseal leak at Turkey Point was reportedly a small contributor to a total unidentified leakage rate of 0.45 gpm for an operating period of 43 days. This leakage, dripping onto the top of the head deposited an estimated 40-60 pounds of boric acid and resulted in a loss of material over a 8.5 x 1.5 inch area, approximately 0.25 inches deep. Although not due to nozzle leakage, these cases demonstrate that significant corrosion of the head can occur at high temperatures whenever deposits remain moist.

#### **PWSCC Cracks in B&W Design PWR Plants**

The most directly related experience has been cracking and leakage of CRDM nozzles at the other B&W design plants: Arkansas Nuclear One Unit 1 (ANO 1), Crystal River 3, Oconee 1-3, and Three Mile Island Unit 1 (TMI 1). All of these units have experienced cracks and leaks from the nozzles near the J-groove weld elevation. The cracks have been predominately axial and have tended to initiate on the outside surface of the nozzle at the weld toe or in the weld. In some cases, there have been circumferential cracks in the nozzle wall above and below the J-groove weld.

Laboratory examination of specimens removed from Oconee 1 and Oconee 3 confirmed that the axial cracks (Oconee 1) and circumferential cracks above the J-groove weld (Oconee 3) were PWSCC.

Figure 16 shows the locations of the leaking nozzles in the B&W design plants. It should be noted that the leaking nozzles are distributed across the RPV head. Figure 17 provides further information regarding the distribution of leaking nozzles. This figure shows the fraction of all of the nozzles at each row that have leaked and whether the cracks are purely axial or axial with circumferential cracks above the J-groove weld elevation.

#### **Lack of Fusion in J-Groove Welds**

During a CRDM nozzle inspection at Ringhals Unit 2 in 1992, an indication was detected in the J-groove weld at one of the penetrations. The indication was not indicative of PWSCC; rather, the indication was attributed to a weld defect that occurred during fabrication of the CRDM nozzle to the RPV head. The B&WOG took action to address this concern by acquiring additional data from several sources. First, the data from Ringhals Units 2 and 4 and data from a cancelled Westinghouse reactor, Shearon Harris, were acquired from the Westinghouse Owners Group (WOG). Second, the B&W Owners Group (B&WOG) performed an inspection of the RPV head from Midland Unit 1, which was a cancelled nuclear station fabricated by B&W.

An addendum to the B&WOG safety evaluation was prepared to analyze these data (reference 8.2.9). This evaluation included a statistical review and analysis of the J-groove weld inspection data and a stress analysis of the CRDM J-groove weld to determine the minimum weld area that is required to meet the American Society of Mechanical Engineers (ASME) Boiler and Pressure Vessel (B&PV) Code primary shear stress limits. It was shown in this report that the maximum areas of weld lack of fusion detected for the Midland Unit 1, Shearon Harris, and Ringhals Unit 2 RPV heads are well below the ASME Code allowable limits for weld structural integrity. It was concluded that a large margin exists between the statistical bound of the total lack of weld fusion areas in the Midland Unit 1 RPV head and the ASME Code allowable limits. Therefore, although some areas of lack of fusion are expected to be observed, they do not give rise to a safety concern.

#### **Comparison of Davis-Besse Nozzles to Other B&W Design Plants**

Table 6 is a comparison of key features of the Davis-Besse RPV head to the other B&W design plants from the standpoint of cracks and leaks. This table shows several potentially significant design and fabrication differences.

##### Operating Temperature

The Davis-Besse operating condition RPV head temperature is reported to be 605°F relative to the 601-602°F for the other six B&W design plants. This small temperature difference has some effect on the predicted time to leakage, and this fact is reflected in the row which reports the EFPYs adjusted to a common 600°F operating RPV head temperature. The effect of the higher Davis-Besse RPV head temperature is offset by the shorter operating time, leading to a temperature adjusted time that is less than Oconee 1, 2 and 3, and ANO 1.

##### Counterbores at the Top and Bottom of CRDM Nozzles

All of the B&W design plants except for Davis-Besse were designed with a counterbore machined into the penetration hole in the RPV head before installing the CRDM nozzles. Elastic-plastic finite element stress analyses show little difference in welding residual and operating stresses for the two designs, especially for nozzles near the center of the RPV head

where the counterbore is only a short distance above the top of the J-groove weld. Therefore, the lack of a counterbore in the Davis-Besse's design is not considered to be a factor in the condition.

RPV Head to Hot Leg Vent Line at CRDM Nozzle 14

Davis-Besse has a vent line that runs from nozzle 14 to the steam generator 2 upper primary hand hole. This line is unique to Davis-Besse. The purpose of the line is to vent non-condensable gases from the head during a loss of coolant accident. This vent line could have a minor effect on head temperature. However, since this nozzle is displaced from the cracked nozzles, its effect on other nozzles is considered to be very small. There is no evidence of thermal fatigue on this penetration.

Susceptibility of Davis-Besse CRDM Nozzles to PWSCC

The 69 CRDM nozzles in the Davis-Besse RPV head were manufactured from four different heats of material as shown in the following table (reference 8.2.1). Three of the heats (C2649-1, M3935, and M4437) of material were manufactured by B&W Tubular Products (B&W-TPD), and the fourth heat was manufactured by the International Nickel Corporation (INCO). According to an assessment performed by Framatome ANP, these CRDM nozzles have a relatively high susceptibility to PWSCC, mainly because of the residual stress distribution calculated in the vicinity of the J-groove weld and the Davis-Besse RPV head operating temperature of 605°F (reference 8.2.2).

**CRDM Nozzle Heats at Davis-Besse**

Heat Number	No. of Nozzles	YS (ksi)	UTS (ksi)	Carbon (%)	Anneal Temp (F)	Nozzle Nos.
C2649-1	32	44.9	92.6	0.042	1600-1700	7, 12, 16, 20, 22-25, 27-29, 38-44, 47-55, 57, 64, 65, 68, 69
M3935	5	48.5	85.6	0.028	1600-1700	1-5
M4437	23	35.9	92.2	0.059	1600-1700	8-10, 13-15, 17-19, 21, 26, 30-37, 61-63, 67
NX5940	9	39.0	83.0	0.030	1600 min.	6, 11, 45, 46, 56, 58-60, 66

Experience to date has shown that:

- There are more leaks (15) from nozzles fabricated from heat M3935 than any other single heat (4 max) in B&W design plants, and
- A larger fraction of nozzles (20.3%) from heat M3935 have developed leaks than any other single heat (13.3% max) in B&W design plants.

Nozzles 1 through 5 at Davis-Besse are from heat M3935. Nozzles 1, 2 and 3 have through-wall axial cracks and leaks with nozzle 2 having notable RPV head corrosion and nozzle 3 having extensive corrosion. In addition, nozzle 5 had an axial crack requiring repair. Nozzle 47 also had an axial crack requiring repair, but the nozzle was from heat C2649-1. In

summary, the leaks at Davis-Besse are all from the heat of material that has previously resulted in more leaks than any other heat in the industry.

#### Range of Interference Fits

Davis-Besse is similar in design to Oconee, Crystal River-3, TMI 1 and ANO 1, which have demonstrated an ability to identify leaking CRDM nozzles through an interference fit by visual inspection for boric acid crystal deposits. During fabrication, CRDM bores were inspected for final top and bottom bore diameter and verticality. After custom grinding individual CRDM nozzle shaft to approximately 0.001" greater in diameter than the final CRDM bore diameter, the shafts were measured at both the top and the bottom of the custom ground length. CRDM nozzle shafts are longer than CRDM bores are deep. Thus, CRDM nozzle shaft diameter measurements do not directly line up with CRDM bore diameter measurements, although in the case of Davis-Besse these locations should be fairly close because of the lack of counterbores. Therefore, the resulting top and bottom dimensional fits are considered approximate. The values for the Davis-Besse RPV head are calculated to range from a gap of 0.0010" to a maximum interference fit of 0.0021".

#### **High PWSCC Susceptibility in Heat M3935**

The reason for the higher susceptibility of heat M3935 has not been determined although it may be related to a lower than optimum annealing temperature or through-thickness hardness gradient created in the material by a forming operation after annealing. Additional data will be acquired during examinations of nozzle 3 (see section 7.3.3). However, this data is not needed to support the basis of this root cause document.

While heat M3935 appears to have higher PWSCC susceptibility than some other heats, several other heats of material have also experienced multiple leaks in B&W design plants. Heats of material that have not experienced leaks to date may experience cracks and leaks in the future. The same is true for J-groove welds.

#### **Other Possible Causes of Cracks**

Several other potential mechanisms for crack initiation and propagation were considered for the observed flaws in the CRDM nozzles. These are:

##### Fabrication and Inspection Anomalies

All the CRDM nozzle Alloy 600 materials used by B&W during the Davis-Besse RPV head manufacturing were either supplied by the B&W-TPD or by INCO. The materials were ordered to ASME Boiler and Pressure Vessel (B&PV) Section II Specification SB-167 and Section III requirements. Any fabrication or inspection anomalies would have been identified since dye penetrate testing (PT and UT was performed).

##### Thermal Fatigue

CRDM nozzles may be subject to thermal fatigue induced by thermal fluctuations, which result from particular operating transients. Several permutations of stratified fluid conditions have been observed to result in fatigue cracking and component failures in PWRs. However, no CRDM nozzles have experienced this type of failure, and there is no historical evidence to support thermal fatigue cracking. Given the past experience, it seems unlikely that thermal fatigue degradation would result in the formation of discrete axial cracks located at high stress locations (uphill and downhill sides) within the bore of the CRDM nozzles.

### Intergranular Stress Corrosion Cracking (IGSCC)

Cracking can possibly occur due to additional factors not normally associated with PWSCC. Contaminant species such as sulfur, chloride, or fluoride compounds could result in IGSCC. Oxygen at levels found in boiling water reactors also can cause IGSCC. The presence of these contaminants in combination with high stress and less than ideal material microstructure could lead to IGSCC. However, there is no evidence that this occurred at Davis-Besse (see following section). In PWRs, there is insufficient oxygen to cause IGSCC. Davis-Besse has not experienced any incidents of resin ingress, which is the most common source of sulfur (Reference 8.2.1). Also, chlorides and fluorides are controlled in the primary water. Thus IGSCC is discounted as a failure mechanism since oxygen, chlorides, fluorides or sulfur were not present in sufficient quantities in the reactor coolant system (RCS).

### RCS Chemistry Control

Chemical transients in the primary water were considered to determine if nozzle cracking was influenced by conditions other than those causing PWSCC. In response to Generic Letter 97-01, Framatome report BAW-2301 (reference 8.2.1) summarized abnormal chemistry time periods at each of the B&WOG plants. The primary water chemistry analysis results at each of the B&WOG plants were reviewed for excursions during power operation, hot shutdowns, and cold shutdowns. At the time of this report, no events have occurred at Davis-Besse since December 10, 1983 when a resin specification problem led to a short transient in chlorides (up to 0.26 ppm) and lithium. This event is not considered significant.

The amount of hydrogen in the primary coolant during the last three cycles was analyzed to confirm that excess oxygen was not available to promote corrosion within the primary side.

Boric acid quality was researched as a possible issue, and potential for impurities to contribute to nozzle cracking. It was determined that the boric acid used at Davis-Besse is common to the industry and that the quality control program in place for the boric acid is appropriate. Additionally, pure boric acid with no impurities has been shown in the Boric Acid Corrosion Guidebook (reference 8.5.2 or 8.5.3) to be capable of the corrosion rates seen in this condition.

### Other Failure Mechanisms

Other failure mechanisms were considered briefly and discarded since either they would already be encompassed by the environmentally assisted mechanisms noted above or the review of the evidence did not support them. These include environmentally assisted fatigue, mechanically induced fatigue, and hydrogen damage.

### Conclusions Regarding Source of Cracks

The similarity of the flaws in the Davis-Besse CRDM nozzles 1, 2, 3, 5, and 47 to the PWSCC cracks found at the other B&W designed nuclear power plants supports the evidence for concluding that the flaws are PWSCC. The flaws are similar in length and orientation to confirmed PWSCC at other plants and there is no other credible mechanism for these types of flaws. Four of the five cracked nozzles at Davis-Besse, and all three of the leaking nozzles at Davis-Besse, are from heat M3935 that has exhibited the highest percentage of leakage of any heat of material in domestic PWR plants. Therefore, the probable cause of cracks in the Davis-Besse nozzles is PWSCC.

### **Crack Propagation to Leak**

PWSCC of Alloy 600 components in RCS can lead to through-wall cracking, and, thus, leakage of primary water. Based on the visual inspections of the Davis-Besse RPV head, containment air cooler cleaning frequency, interviews, etc., a reasonable time-frame for the appearance of leakage on the RPV head at Davis-Besse is approximately 1994-1996. Utilizing an average PWSCC crack growth rate of approximately 4 mm/year (reference 8.5.9) through the 16 mm (0.62 inch) thick CRDM nozzle material, the time-frame at which crack initiation occurred would correspond to approximately  $1990 \pm 3$  years. This is a reasonable approximation to the more detailed type of calculations performed by the B&WOG in the safety assessment (reference 8.5.5), which assumes approximately 4-6 years for a through-wall flaw to develop in the area near the J-groove weld.

### **3.2.2 Leakage Rate From CRDM Nozzle Cracks**

Nozzles with through-wall PWSCC cracks in either the nozzle wall or J-groove weld can develop leaks into the annulus between the nozzle and hole in the RPV head. The following is a discussion of Davis-Besse and industry experience regarding leak rates.

#### **Industry Experience**

Prior to Davis-Besse, reported industry experience had been that PWSCC cracks at RPV head nozzle penetrations only result in a small ring of boric acid crystal deposits as shown in Figure 18. Estimates from Oconee are that the volume of deposits from these leaks is less than 1 in<sup>3</sup>. Using Figure 6-3 of the Boric Acid Corrosion Guidebook, Revision 1 (reference 8.5.3), and an assumed average boron concentration of 750 ppm over an operating cycle, one cubic inch of boric acid corresponds to leakage of about 1 gallon of water. This corresponds to an average leak rate of about  $1 \times 10^{-6}$  gpm over an operating cycle (two year period).

Low leak rates have been reported for most other nozzles attached by J-groove welds including pressurizer instrument nozzles, pressurizer heater sleeves, and hot leg piping instrument nozzles. However, there have been some cases where larger leakage has been reported. These cases include a pressurizer heater sleeve containing a failed heater (ANO 2), and several piping instrument nozzles (ANO 1 & Palo Verde 2). In summary, while most through-wall cracks at Alloy 600 nozzle attachment welds result in very small leaks, there are exceptions where greater leakage has occurred.

There are several main theories that explain why leak rates are typically low.

- The cracks only extend a short length in the high tensile residual stress zone above the J-groove weld.
- PWSCC cracks are tight and may become plugged by small amounts of impurities in the primary coolant.
- The leaking fluid flashes within the crack, leaving boric acid deposits that block further flow through the crack.

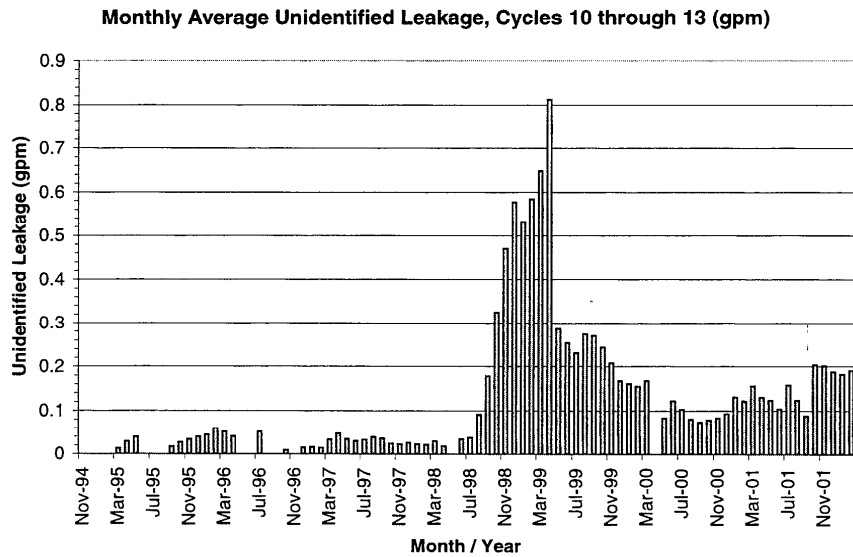
The most likely explanation is that low leakage results from tight PWSCC cracks that extend a short distance above the J-groove weld. The basis is that low leakage is also observed from most smaller diameter instrument nozzles that are also installed in pressure boundary parts by J-groove welds without an interference fit.

While the exact cause of the previously observed low leak rates has not been conclusively established, it has been determined that the leak rates are typically low, and qualified visual

inspection programs are required to identify the leaks. A "qualified visual inspection" requires 1) a clean enough RPV head to identify small rings of boric acid crystal deposits, 2) visual access to locations where nozzles penetrate the RPV head, and 3) confirmation that there will be a flow path through the annulus between the RPV head and nozzle under operating conditions. Because an interference fit was predicted, Davis-Besse could not "qualify" nozzles 1-5 for a visual exam, whether or not they were clean. However, because of the very small percentage of actual metal-to-metal interference (i.e., high points only) leakage is anticipated despite the predicted interference.

**Unidentified Primary System Leakage Rates at Davis-Besse**

Normal operational leakage in the RCS is recorded and analyzed in MODES 1-4, looking for adverse trends and to verify compliance with Technical Specification 4.4.6.2. This Technical Specification requires that there is no pressure boundary leakage, and that unidentified leakage is maintained at less than 1 gpm. Although the surveillance is required once per 72 hours, RCS leakage is generally trended once per day. DB-SP-03357, RCS Water Inventory Balance, provides the methodology to determine the RCS leakage rate. The test calculates total RCS leakage by resolving changes in initial and final values of Pressurizer and RCS Makeup Tank levels over a 1 to 4 hour period, and providing corrections based on RCS temperatures and pressures. Identified sources of leakage that are apparent through changes in Pressurizer Quench Tank level, normal (measured) Reactor Coolant Pump seal leakage, or quantified primary to secondary tube leakage, are subtracted from the calculated total RCS leakage to obtain the unidentified leakage value. This method of determining unidentified leakage has a significant daily variation (in the range of 0.05 to 0.1 gpm) that depends on accuracy of identified leakage measurements, stability of the plant during data collection, and duration of data collection. Therefore, monthly or running averages are most useful to determine leakage trends, similar to that presented in the figure below.





During operating cycles 10 through 13 (November 1994 through February 2002), measured unidentified leakage has ranged from slightly negative to as much as approximately 0.8 gpm in April 1999. From review of data over that time span, it would appear that average unidentified leakage tends to be in the range of 0.0 to 0.03 gpm when the plant is "tight" with no pending maintenance concerns. If unidentified leakage begins to trend upward, efforts are expended to determine the cause, and if necessary, effort is made to repair the source of the leakage. For example, the high leakage in April 1999 was identified as from the Pressurizer Code Safety Valves and the plant was shutdown to service the valves. Following that shutdown, unidentified leakage remained in the range of 0.15 to 0.25 gpm, some of which was attributable to CRDM flange leakage and some of which may have been attributed to CRDM nozzle leakage.

When a CRDM nozzle begins to leak, experience has shown that one of the first signs is the appearance of a small boric acid deposit crust at the base of the CRDM flanges where it emerges from the RPV head. To put nozzle leakage in perspective, a leak rate of 0.00001 gpm could deposit 10 cubic inches of boric acid over the course of a fuel cycle, which would be quite visible on a clean RPV head. Compared with unidentified leakage of a "tight" RCS at 0.03 gpm, it is apparent that unidentified leakage measurements cannot be used to detect early through-wall leakage at a CRDM nozzle. Figure 19 shows the unidentified leakage rate over cycle 13. It is possible that the approximately 0.10-0.15 gpm increase in unidentified leakage starting in October 2001 is related to changing conditions at the crack in nozzle 3. Subtracting a base leakage rate of 0.05 gpm from the total unidentified leak rate in Figure 19, the maximum leakage rate from the CRDM nozzles did not exceed 0.15- 0.20 gpm at any point in time.

In summary, RCS leakage is at best a late-term indicator of leaking CRDM nozzles. By the time RCS leakage can be used directly, there is a potential for advanced corrosion of the low-alloy steel RPV head.

#### **Predicted Leak Rates from PWSCC Cracks**

Dominion Engineering, Inc. Calculation No. C-5509-00-6 (reference 8.2.4) provides predicted leak rates from nozzles with PWSCC cracks. Key results are plotted in Figure 21. The basis for these leak rates are as follows:

##### Length of Cracks in Davis-Besse Nozzles 2 and 3

The longest crack lengths above the top of the J-groove weld determined by UT measurements are 1.1" for nozzle 2 and 1.2" for nozzle 3. The longest cracks above the J-groove weld previously discovered in other plants with low observed leakage are <1.0 inch. Since the Davis-Besse cracks are longer than in other B&W design plants, higher leak rates would be expected.

##### Leakage From an Axial Crack in a Pipe

Cracks above the J-groove weld can be modeled as through-wall axial cracks in a straight length of pipe subjected to internal pressure. The model used for the results plotted in Figure 21 is based on crack opening areas from the EPRI Ductile Fracture Handbook (reference 8.5.6). Leak rates are computed from the crack opening area using models developed by EPRI [Steam Generator Integrity Assessment Guidelines: Revision 1 (reference 8.5.7), and PWR Steam Generator Tube Repair Limits: Technical Support Document for Expansion Zone PWSCC in Roll Transitions (reference 8.5.8)].

The predicted leak rates are 0.025 gpm for the 1.2" crack at Davis-Besse nozzle 3, 0.018 gpm for the 1.1" crack at nozzle 2, and about 0.012 gpm for the longest previously encountered crack. These results show higher predicted leak rates for the longer Davis-Besse cracks and

that the total predicted leak rate is significantly less than the 0.1-0.2 gpm inferred from the measured unidentified leak rate.

#### Effect of J-Groove Weld on Crack Opening Area

The finite element model in Figure 15 shows the hoop stresses in the nozzle including the effects of welding residual stresses and operating pressure and temperature. The tensile hoop stress shown in the area of the J-groove weld will tend to open a crack at this location.

The finite element model shown in Figure 15 was modified by releasing the nodes on the plane of symmetry in the area of the axial crack as shown in Figure 22 and described in Dominion Engineering, Inc. Calculation No. C-5509-00-7 (reference 8.2.5). The resultant crack opening displacements shown in Figure 23 result in a predicted leak rate of over 1 gpm for the 1.2" long crack at nozzle 3.

An additional load step was added to the model to simulate the loss of low-alloy steel from behind the J-groove weld. Removal of the constraint provided by this material resulted in the crack closing up somewhat and a predicted leak rate of about 0.8 gpm for the 1.2" long crack in nozzle 3.

The above analyses illustrate the potential for leakage rates ranging from 0.025 gpm for the case of a 1.2" long axial crack in a straight run of nozzle material remote from the weld to 1 gpm or more for the case where weld shrinkage forces act on a long crack that extends 1.2" above the top of the J-groove weld.

#### Estimated Leak Rate Based on Boric Acid Deposits on RPV Head at 13RFO

An alternate means to estimate leak rates for this condition would be from boric acid accumulations. Because of uncertainties in how much boric acid left the head region, this method is only useful as a comparison. Figure 20 shows boric acid deposits on the RPV head prior to cleaning at 13RFO. The volume and weight of these deposits are estimated to be 11.5 ft<sup>3</sup> and 900 lb at an assumed density of 1.25 g/cc (reference 8.2.13), which is about midway between the density of boric acid crystals and powdered boric acid. Assuming that the average boron concentration in the primary coolant is 750 ppm, Figure 6-3 of Boric Acid Corrosion Guidebook, Revision 1 (reference 8.5.3) shows that 900 lb of boric acid deposits are the result of about 20,000 gallons of water. Assuming a linearly increasing leak rate over a two-year period of time, the maximum leak rate at the end of three years would be about 0.04 gpm. However, a substantial (but unquantified) amount of boric acid appears to have been drawn out of the CRDM service structure by the CRDM ventilation system and deposited in containment (CTMT). Thus, the leakage estimate may be low. More specifically, 10 ft<sup>3</sup> of wet boric acid were removed from the containment air cooler plenum during 13RFO. While this is almost as much material as was found on the RPV head, it is important to realize that the total unidentified primary leakage during cycle 13 was more than 0.1 gpm. It is not likely that all of this leakage was from nozzle cracks on the RPV head. Therefore, the estimate, 0.04 gpm, based on 900 lbs. of boric acid is a minimum predicted leakage rate from the nozzle cracks.

#### Conclusions Regarding Leak Rate From PWSCC Cracks

The unidentified leakage during late 2001 attributed to CRDM nozzle leaks (0.1-0.2 gpm) is bracketed by the predictions based on leakage from an axial crack in a pipe (0.025 gpm) and the finite element analysis of crack opening area at the J-groove weld elevation after corrosion of the low-alloy steel material (0.8 gpm). Further refinement of the predicted leak rate is not possible due to the significant uncertainty regarding the exact shape of the crack in the nozzle wall and in

the J-groove weld. However, the analyses clearly demonstrate the potential for significant increases in flow rate as the crack grows in length.

### **3.2.3 Source of Boric Acid Deposits on RPV Head**

As shown in Figure 24 there were extensive boric acid deposits on the RPV top head surface at the start of 13RFO. These deposits are considered to have come from two main sources, leakage from CRDM nozzle flange joints (uncleaned from previous cycles) and leakage from PWSCC cracks at nozzles 2 and 3.

#### **Leakage From CRDM Nozzle Flange Gaskets**

Figure 3 shows a typical CRDM flanged joint in a B&W-design plant. The joint consists of an Alloy 600 nozzle welded to the underside of the RPV head by a J-groove weld, a stainless steel flange welded to the Alloy 600 nozzle, a flange on the CRDM, two spiral wound gaskets, two 180° split nut ring segments below the flange and eight bolts.

Leakage from the CRDM flange gaskets was experienced early in life at B&W designed plants. Leakage from the flanged joints sometimes resulted in formation of concentrated boric acid on the flange with resultant corrosion of the originally installed low-alloy steel nut ring segments. One such condition at ANO 1 in 1989 is described in the Boric Acid Corrosion Guidebook (reference 8.5.2). During the 1980's and 1990's, the gaskets were changed to graphite/stainless steel (SST) spiral wound gaskets and the split nut ring was changed to a corrosion resistant SST material.

#### **Leakage from Davis-Besse CRDM Nozzle Flange Gaskets Prior to 13RFO**

It is reported that graphite/SST gaskets and corrosion resistant nut rings were installed at Davis-Besse over several outages.

- 6RFO Replaced 23 gaskets
- 7RFO Replaced 15 gaskets
- 8RFO Replaced 14 gaskets
- 9RFO Replaced 8 gaskets
- 10RFO Replaced 9 gaskets

It has been reported by Framatome that Davis-Besse is the only plant to have experienced leaks with the new gaskets and bolting materials. Specifically,

- 8RFO Replaced gasket on nozzle 66 (a minor leaker)
- 11RFO Small leak detected at nozzle 31 (was not repaired)
- 12RFO Nozzle 31 identified as leaker and repaired. Nozzles 3, 6, 11, and 51 identified as possible leakers and gaskets replaced
- 13RFO No flange leaks identified

The largest of these leaks was from nozzle 31 at 12RFO. It is reported that steam cutting had occurred and that flange repairs were required in addition to just replacing the gasket.

#### **Source of Boric Acid Deposits on Davis-Besse RPV Head**

It is considered that most of the boric acid deposits found on the Davis-Besse RPV head at 13RFO have come from leaking nozzle 3 with potential contributions from nozzle 2. The basis is that the vessel head was reported to be clean at 9RFO, significant boric acid deposits had appeared on the vessel head by 11RFO, there were no significant gasket leaks prior to 11RFO, experience in the industry does not suggest that leakage from the nozzle 31 flange gasket would

have resulted in extensive deposits on the vessel head at 12RFO, and additional deposits appeared during cycle 13 when there were no reported flange leaks.

The source of the deposits is further supported by the reactor head boric acid sample results reported in reference 8.2.14 and described previously in section 3.1.5 of this report.

#### **Volume of Boric Acid Deposits on Davis-Besse RPV head at 13RFO**

The volume of boric acid deposits on the RPV head at 13RFO is estimated in a Dominion Engineering, Inc. calculation (reference 8.2.13). The approach used was to divide the RPV head into sixteen areas, estimate the depth of deposits in each area by reviewing inspection videotapes, and then calculate the weight of deposits in each area using the area, depth of coverage for each sector, plus an assumed density midway between that of solid boric acid and loose boric acid crystals. The worksheet calculations show an estimated volume of 11.5 ft<sup>3</sup> and a weight of 900 pounds.

In summary, while the case is not conclusive, it is probable that the approximately 900 pounds of boric acid deposits that accumulated on the RPV head are the result of leakage from the PWSCC crack at nozzles 2 and 3.

#### **3.2.4 Corrosion of RPV Top Head Surface**

As shown in Figure 6, the RPV top head surface was corroded. During this investigation, attention was focused on boric acid corrosion as the source of the large volume of material loss downhill from nozzle 3. The potential for boric acid corrosion of low-alloy steel RPV heads has been known since the mid-1980's and there is no other plausible explanation for loss of this much material.

#### **Historical Perspective on Boric Acid Corrosion of PWR Primary System Components**

The potential for boric acid corrosion of PWR primary loop components has been recognized since the plants were designed. Several incidents between the late 1970's and the mid 1980's led to the NRC issuing Generic Letter 88-05, Boric Acid Corrosion of Carbon Steel Reactor Pressurizer Boundary Components in PWR Plants (reference 8.3.1). EPRI issued the original Boric Acid Corrosion Guidebook in 1995 (reference 8.5.2), and the guidebook was revised in 2001 (reference 8.5.3). The later document includes summary descriptions of more than 100 incidents including corrosion of RPV heads, high pressure injection nozzles, reactor coolant pump studs, etc.

#### **Previous Boric Acid Corrosion of RPV Top Head Surfaces**

Prior to the current condition at Davis-Besse, the greatest reported quantity of boric acid deposits on a RPV head was over 500 pounds at Turkey Point 4. These deposits were kept wet from a leak rate of less than 0.45 gpm (from a Conoseal leak). Corrosion on the RPV head was relatively minor, (approximately 0.25 inches depth).

There was corrosion of the low-alloy steel bottom head of a Combustion Engineering pressurizer at ANO 2 in 1987. In this case, a leak of about 0.002 gpm over less than six months time resulted in a corroded area about 1.5 inches in diameter and 0.75 inches deep. This leak resulted from a crack in an Alloy 600 sleeve associated with swelling of a failed Alloy 600 heater inside the sleeve.

### **Estimated Corrosion Rates at Davis-Besse Nozzle 3**

The volume of material lost at the cavity between nozzles 3 and 11 was estimated to be about 125 in<sup>3</sup> giving a weight loss of approximately 35 pounds.

Review of the sequence of relevant events in Attachment 2 suggests that the corrosion rate began to increase significantly starting at about 11RFO and acted for a four year period of time. With the maximum corrosion length of about 8 inches between nozzles 3 and 11, the average corrosion rate would be about 2.0 inches/year. As a bounding assumption, if the rate increased linearly with time, the maximum corrosion rate near the end of Cycle 13 would be about 4.0 inches/year. The rates growing laterally from the main axis of the cavity would be about half of the rates growing axially, or 1.0 to 2.0 inches/year.

Figure 25 from the Boric Acid Corrosion Guidebook, Revision 1 (reference 8.5.3) summarizes the available test data regarding boric acid corrosion. These data show that most of the data points for borated water dripping onto hot metal surfaces, impinging onto hot metal surfaces, or leaking into a heated annulus, are in the range of 1.0 to 5.0 inches/year. This is consistent with the observed conditions.

Further effort is ongoing to better define the corrosion rates based on the final measured size of the cavity and thermal-hydraulic modeling being performed by the MRP. Technical insights gained from that effort may provide improved understanding, but are not expected to conflict with the evidential basis for the projections made here.

### **Progression from Initial Small Leak to High Corrosion Rates**

An important issue is why some of the leaking CRDM nozzles (especially nozzle 3) at Davis-Besse progressed to a high leak rate and corrosion while leaks at the six other B&W design plants have remained small. Several possibilities were explored.

#### **Crack Grows Longer With Time**

One possibility is that the axial PWSCC crack simply grows longer with time and this increases the leakage rate. Prior to Davis-Besse, the greatest crack extension above the J-groove weld was just under 1 inch. The longest cracks at Davis-Besse extend 1.1" above the top of the J-groove weld at nozzle 2 and 1.2" above the top of the J-groove weld at nozzle 3.

#### **Corrosion Begins Deep in Annulus and Increases With Time**

It is likely that corrosion initiates deep within the crevice and progresses to the surface as indicated by the corrosion at nozzle 2. This would be consistent with a test conducted by Southwest Research Institute for EPRI and described in the Boric Acid Corrosion Guidebook, Revision 1 (reference 8.5.3). However, for there to be significant boric acid corrosion below the surface, there would have to be evidence of boric acid crystal deposits at the annulus outlet. Since other plants have not reported significant boric acid crystal deposits around the annulus this model does not explain the difference.

#### **Boric Acid on Top of RPV Head Acts as Incubator or Insulator**

Laboratory test experience with bolted flanges has demonstrated that corrosion rates can increase for conditions where leaking borated water is retained in a bolted flanged joint by insulation or a loose fitting band. Boric acid deposits on the RPV head from other sources, such as leakage from CRDM flange joints, could possibly provide the same type of "incubator" as insulation on flanged joint. However, this is only expected to be a short term "head start" since leakage of borated water from a PWSCC crack will eventually create its

own boric acid deposits at the annulus which would behave the same as boric acid from flanged joints.

### **Morphology of the Affected Area as Damage Progresses**

Based on the investigations of the root cause team, it is clear that leakage from PWSCC cracks was a necessary precursor to the material loss adjacent to nozzles 2 and 3. These leaks led to local environmental conditions that produced modest material loss around nozzle 2 and much more extensive degradation around nozzle 3. The main effect of the leakage was to provide a boric acid solution that concentrated through boiling heat transfer along the leak path. Provided that sufficient levels of oxygen are available—either directly or remotely through a crevice corrosion mechanism—the concentrated liquid boric acid solution may cause relatively high corrosion rates up to on the order of four inches per year. A possible secondary effect of the leakage is to enhance the material loss of the low alloy steel through flow-related mechanisms. These mechanisms are flow accelerated corrosion (FAC), droplet and particle impingement erosion, and potentially steam cutting.

Given the current limited experimental data applicable to the observed degradation and the lack of existing detailed analytical calculations of the thermal-hydraulic and thermochemical environment along the nozzle leak path, it is not possible to definitely state the exact progression of mechanisms that led to the observed material loss. The environment along the leak path—from the primary system pressure inside the CRDM nozzle, through the axial PWSCC crack extending above the top of the J-groove weld, up through the annulus or cavity on the periphery of the nozzle, and then out to the ambient pressure above the top head surface—is the result of complex processes such as critical two-phase flow, two-phase frictional and acceleration pressure drops, boiling heat transfer, boiling point elevation due to boric acid solution concentration, oxygen and hydrogen transport, various electrochemical processes, convective heat transfer on the surfaces of the head, and conduction heat transfer within the head materials. Therefore, a detailed description of the damage progression including the precise physical mechanisms with a quantitative breakdown of the relative importance of each mechanism would be speculative.

However, the degradation modes on the two extremes of the overall progression are known with reasonable confidence, and some conclusions can be made regarding the possible modes of degradation in between these two extremes. The first extreme is associated with the lack of material loss and extremely small leak rates observed for most of the leaking CRDM nozzles in the industry. For these extremely low leakage rates (on the order of  $10^{-6}$  to  $10^{-5}$  gpm) the leaking flow completely vaporizes to steam immediately downstream of the principal flashing location, most likely at the exit of the PWSCC crack. The result is to keep the gap between the nozzle and head dry, precluding high rates of low alloy steel material loss. In addition, the small velocities associated with the extremely small leakage preclude the flow mechanisms from being active.

The other extreme of the degradation progression is associated with the large cavity located adjacent to nozzle 3. For this cavity, it is clear that the degradation proceeded by the classic boric acid corrosion mechanism associated with liquid boric acid solution concentrated through boiling and oxygen directly available for corrosion from the ambient atmosphere. The magnitude of the boiling heat transfer associated with the relatively high leak rate of nozzle 3 is sufficient to cool the head enough to allow liquid solution to cover the walls of the cavity.

In between these two extremes, increase in the extent of the axial PWSCC crack above the top of the J-groove weld resulted in increasing rates of leakage for nozzle 3. It is likely that the degradation proceeded at relatively low rates by an erosion mechanism, enhanced to some degree

by galvanic corrosion associated with the dissimilar metal couple of the Alloy 600 nozzle and low alloy steel head material.

While it is not possible within current knowledge to definitively identify a progression of corrosion mechanisms, the overall effect and cumulative timeframe is apparent. Linking the corrosion mechanisms that were described above (with some supplemental understanding), it is possible to construct a "viable" progression of events.

#### Stage 1 - Crack initiation and progression to through wall

First, based on the body of knowledge available, a crack initiated in nozzle 3 at around 1990 ( $\pm 3$  years) due to PWSCC. The crack grew at a rate consistent with industry data, progressing to a through-wall crack that penetrated above the J-groove weld in the 1994 to 1996 time frame. At this point the RCS leakage would have been miniscule, and in no way detectable by any currently installed leakage monitoring system.

#### Stage 2 - Minor Weepage / Latency Period

Leakage would have entered the annular region between the Alloy 600 nozzle and the low-alloy steel base material of the RPV head. However, the interference fit that was initially expected in nozzle 3 is composed of only about 5 percent of actual metal-to-metal high point contact. At its tightest, the rest of the interface is essentially an annular "capillary" flow path. Even if the flow path could not actively leak, it would still be permeated with moisture from the newly developed crack. With addition of moist boric acid in this bi-metallic annulus, several forms of boric acid corrosion are possible, in addition to galvanic attack. These corrosion mechanisms would open an annular gap, if it did not previously exist, and allow leakage flow to the surface. If the RPV head had been initially clean, and if a timely 100% bare head visual inspection had been completed, the leakage would most probably have expressed itself within a short time as the classical "popcorn" crust of boric acid deposits. This would have been apparent within one or two fuel cycles from the time the crack progressed through the nozzle wall and would not have been accompanied by large scale corrosion of the low-alloy steel. However, at Davis-Besse, the "popcorn" manifestation was not yet observed, and its detection could have been obscured by previous flange leakage deposits.

Given time, the crack continued to grow, leakage increased, and the annular gap increased in width. With an ever widening gap, oxygen may begin to enter the annulus, thus accelerating boric acid corrosion in the gap and diminishing the relative importance of galvanic corrosion. However, due to restriction of oxygen and moisture, corrosion mechanisms have not been fully accelerated. As observed at other facilities (and also in Davis-Besse nozzle 1, the least advanced of the leaking nozzles), there was widening of the annular gap and development of flow "channels" in the annulus leads to the near certainty that the principle flow resistance would have been due to the dimensions of the crack, and not due to any restriction offered by the annulus. This is also supported by the relatively low crack growth rate (i.e.,  $< 0.2$  inches/year with microscopic opening width) compared to documented boric acid corrosion rates on the order of 0.02 to 0.08 inches per year for similar geometry as cited in the Boric Acid Corrosion Guidebook (reference 8.5.3). Since the growth in annulus width tends to occur over a broad length around the annulus, the annulus flow area increases faster than the crack flow area. Thus, the crack dimensions dominate the flow resistance, and the majority of the pressure drop occurs as effluent traverses the crack. Based on the reactor coolant enthalpy at the RPV head, approximately 45% of the reactor coolant that escapes from the crack flashes upon discharge, the rest is immediately vaporized by heat transfer from the

metal surfaces at this stage. Thus, boric acid is both atomized with the steam and deposited as molten boric acid on the surrounding surfaces, with moisture escaping as steam.

#### Stage 3 – Deep Annulus Corrosive Attack

Toward the end of the latency period, the crack leakage increases. While the annulus is tight, single phase erosion is possible. However, oxygen penetration may be ever more pervasive if the flow area in the annulus has offset increases in leakage due to crack growth. This would cause annulus velocity and differential pressure to decrease, allowing greater inward penetration of oxygen. With a decreased annulus velocity, single phase erosion would decrease, and forms of flow accelerated corrosion, droplet impingement, and flashing induced corrosion could become dominant. It is probable that a small amount of material would be preferentially corroded in the vicinity of the crack, as evidenced by test EPRI-6, modeling of leakage into annular gaps original Boric Acid Corrosion Guidebook (reference 8.5.2). This test was characterized as having excessive oxygen in the supply water, which would be similar in effect to having oxygen supplied by alternative means (i.e., from the top downward). The net effect is that the corrosion rate can be substantially greater in areas of greater velocity. The velocity increase does not need to be sufficient to cause scrubbing of beneficial oxide layers (i.e., erosion-corrosion), rather, it simply needs to maintain a fresh supply of new reactive oxidizing ions in the boundary layer near the corroding metallic surface. The expected pattern was found at nozzle 2, and would be accompanied by copious amounts of boric acid deposits.

The appearance of the corroded low alloy steel in the Davis Besse nozzle #2 bore bears a striking resemblance to that of the post test EPRI-6 test specimens. As pointed out in Reference 8.6.2, the maximum corrosion rates attained in this test program were as much as 2.5 inches/year. However, these tests were not conducted for a long enough duration to determine if the high rates would be sustained after the annulus dimensions substantially increased.

#### Stage 4 - General Boric Acid Corrosion

Progression to this stage is dependent on crack leakage rate. With high leakage rates, the annulus is flooded with an ever increasing amount of moist steam, partially flashing as it exits. Due to the fact that the annulus still exists, basically in the same geometry, any effluent is directed vertically upward. A large amount of discharged boric acid would have already accumulated in the area around the nozzle. With increased leakage, heat transfer from the surrounding metal is no longer sufficient to immediately vaporize the portion of leakage that does not flash (due to its own initial enthalpy and pressure reduction) as it exits the crack. Recent Finite Element heat transfer calculations completed by Dominion Engineering (reported in reference 8.6.2) indicate that a substantial cooling effect is in progress by the time a leakage rate of approximately 0.05 gpm exists. By the time leakage has increased to approximately 0.1 gpm, the metal surface temperature on top of the head will be suppressed to the boiling point due to the large heat flux required to vaporize the leaking coolant. Thus, the principle characteristic of this stage is that the annulus begins to overflow or expel unflashed liquid, causing an area to be wetted underneath the accumulations of boric acid.

General boric acid corrosion on the wet, oxygenated surface of the low-alloy steel RPV head progresses rapidly. Even reductions in reactor coolant system boric acid concentration toward the end of the operating cycle may not diminish the corrosion rate because the concentration at the metal surface is continuously re-supplied by the boric acid that was previously stored. The wetted surface area is dictated by the leakage rate as determined by



crack size and system pressure, the ability of the RPV head to vaporize the liquid via conduction of heat from the interior of the RPV (i.e., it would be vaporized as it runs), and is also affected by the character of surrounding deposits. Calculations at full temperature and pressure indicate that the affected area would be consistent with the amount of leakage that appears to have occurred. Further, since the wetted area would be the result of liquid overflow, it would be expected to be predominantly downhill from the nozzle, leaving the uphill side much less affected, and affecting an oblong area. This is the pattern observed at nozzle 3.

As general corrosion progresses, it would tend to carve out a "bowl" of corroded (or, oxidized) material. Initially, this bowl would gradually increase in surface area as the leak rate from the crack increases. The area in the middle, having been wetted longer, would be slightly deeper. With a sufficient flow rate, the bowl could begin to fill with a saturated boric acid solution. The saturation temperature and consistency in the bowl could be anywhere between that of dilute boric acid (~watery at 212F), to that of moist, molten orthoboric acid ( $H_3BO_3$ ) (viscous at <365F). As the bowl deepens, thermal effects would limit the widening of the bowl, even as leakage incrementally increases. As the bowl deepens, there would be a lesser need for as much projected surface area to transfer the heat. This is because the thermal resistance to heat transfer would continually decrease as the corrosion depth approaches the stainless steel cladding. Further, as the bowl attains a liquid level, lateral heat transfer from the sides would increase the steaming rate, and tend to govern level. A third self-governing effect would be that if leakage increased, decreasing the boric acid concentration in the bowl, the boiling temperature would decrease. This would increase heat transfer (and vaporization rate) by increasing the temperature difference. Heat transfer would also increase due to decreases in viscosity. Thus, with a relatively constant level, the corrosion surface slope might well be expected to be very steep. Finally, when the liquid at the corrosion front reaches the depth of the stainless steel, downward progression ends. At this point the wetted surface would stop its vertical travel and begin to cause undercutting. The height of liquid boric acid would tend to increase with further increases in leakage, unless the increases in diameter due to outward corrosion were sufficient to offset the increases in leakage. This represents the as-found condition of nozzle 3, with steep walls and an undercut nose on the downhill side.

Throughout the majority of this process, being predominantly top-down, the annulus could remain somewhat intact until the approaching general corrosion front overcomes it. This is because the annular region would remain somewhat protected by the upward flow of de-oxygenated water and steam. Thus, flashing effluent from the crack would be directed upward and out of the annulus while the annulus is in place. However, as soon as the low-alloy steel corrosion front is below the elevation of the crack, the effluent would be directed laterally. This would undoubtedly change the degree of atomization of boric acid and affect the particle size of the boric acid carryover late in the process. If this sequence is accurate, the point at which the corrosion depth reached the crack location might have been around May 2001. At that time, the cleaning frequency of containment air coolers (CACs) due to boric acid fouling decreased.

In addition to this construction, the chromium and nickel content of the sample deposits is consistent with a top-down progression of corrosion (see section 3.1.5).

### **Boric Acid Formations on the RPV Head**

The following is a general description of phase changes that boric acid is known to undergo as temperature is increased. This information is being used as part of the MRP modeling effort to develop a consistent model, including boric acid morphology as the corrosion progresses.

When boric acid is left behind by boiling water, it is first deposited as orthoboric acid ( $H_3BO_3$ ). Although solubility of this material is limited at cooler temperatures, near the melting point of 365°F, the solubility in water is infinite. Thus, as boric acid is deposited on the RPV head, it would tend to increase in temperature from that of saturated water (212°F) to 365°F, at which point it is a viscous liquid. In this form it will tend to flow, causing the formations that have been noted. However, even before all the free water is driven out, at around 340°F the  $H_3BO_3$  begins to dehydrate to metaboric acid ( $HBO_2$ ). This is a white, cubic crystalline solid, and is only slightly soluble in cool water. Metaboric acid has a melting point of 457°F, and may tend to form a "crust" on the deposits and formations of orthoboric acid. With further application of heat, the  $HBO_2$  will further dehydrate at approximately 572°F to tetraboric acid ( $H_4B_4O_7$ ). Tetraboric acid is a vitreous solid or white powder, and is water soluble. At the temperatures encountered on the RPV head, all of the above forms can be found, depending on age, contact with the RPV head, and local temperature.

When boric acid accumulates at a leaking nozzle, some flowing of the orthoboric acid would be expected. Boric acid in the cavity formed at nozzle 3 is most likely highly hydrated  $H_3BO_3$ , since moisture is continually supplied. As it was expelled or extruded from the cavity, it would flow, and undergo the above transformations. These transformations would drive off some moisture that could conceivably contribute to corrosion, but this is expected to be a trivial effect. However, experimental data to predict the extent of motion or the degree of corrosion has not been located.

When nozzle 3 was removed, it was reported from the field that the column of boric acid surrounding the nozzle was porous, with winding tube-like channels (at the time still believed to be carbon steel due to the rust color). A small cavity was below the material, where liquid boric acid of lesser concentration presumably drained or washed out during machining for the original aborted repair attempt. The boric acid remaining would have solidified during cooldown, but would be expected to be full of voids and steam tubes to allow venting of the flashing leakage. The appearance of other formations is consistent with expectations of the transformations and crusty appearance.

### **3.3 Investigation of Lead Indicators**

This data analysis section provides a discussion of plant operational and equipment issues that provide possible lead indicators for the subject condition.

#### **3.3.1 Timeline**

An early step in the root cause evaluation was to establish a timeline of key events. The timeline was revised as the data analysis proceeded and the current evolution is shown in Figure 26.

While the timeline was created based on the information that follows, it is presented first so that it can serve as a useful guide to help focus subsequent discussions.

The timeline summarizes the following information:

- Years from 1995 to present
- Operation from Cycle 10 to Cycle 13

- Refueling outages 10RFO through 13RFO including mid-cycle outage during Cycle 12
- Condition of the CRDM flanges, RPV head flange and RPV top head surface at each outage
- RCS unidentified leakage (discussed previously)
- Containment air cooler cleaning operations
- Containment radiation monitor performance and filter cleaning
- The estimated weight of boric acid deposits on RPV head
- Dates of key industry findings and initiatives relative to RPV head condition

### 3.3.2 Sequence of Relevant Events

Attachment 2 is a table of events relevant to the subject condition. This table was used as input to creating the timeline, the logic chart of key decision points and the other potential lead indicators.

Figure 27 is an events and causal factors chart outlining key decision points and other potential lead indicators.

### 3.3.3 CRDM Flange and RPV Head Inspections during Refueling Outages

In the early 1990's, several B&W design plants began cutting openings in the service structure surrounding the RPV head to afford better access to the center top of the RPV head for inspection and cleaning. Framatome ANP (Framatome Technologies, Inc. at the time) provided proposals to Davis-Besse over a period of several years to perform this work. However, Davis-Besse has not installed these openings. Without these openings, the head visual inspection through the mouse holes is hampered in that the pole-mounted camera can only be inserted a finite distance. The curvature of the RPV head impedes seeing the top of the RPV head with this inspection arrangement. Based on review of video by the root cause team in the presence of the inspector during 11RFO, the optical illusion created by the short focal length of the camera, the curvature of the RPV head and the close proximity of the insulation (nominally 2") at the top of the RPV head appears to have potentially led inspectors to believe that the top of the RPV head had been inspected; however, the inspection may have been approximately 1-2 nozzles away from the center of the RPV head.

Framatome provides a tool to inspect CRDM flanges for leakage with two cameras that is lowered down between adjacent flanges. The lower camera is angled up to look under the flanges for boric acid deposits. The upper camera is a straight ahead view of the flange interface. The housing for the cameras is designed to rest on top of the insulation. At this height, the lower and upper cameras are properly positioned relative to the flange.

#### Prior to 1996

During this time frame, B&W had recommended replacing the original CRDM flange gasket with an improved graphite/SST spiral wound gasket to fix leakage problems that all the B&W design plants had experienced. The plant replaced all of the CRDM flange gaskets by 1996. Davis-Besse developed a priority ranking system and replaced a number of leaking flange gaskets each outage based on outage duration rather than 100% repair. The ranking system was developed by the RCS engineer and is as follows:

Ranking System Developed by the RCS System Engineer

Category No.	Description
1	Weepage visible above nozzle at motor tube (MT) interface and/or below the nozzle at the nut ring (N.R.) joint
2	Minimal leakage at M.T. and/or N.R. to nozzle interfaces (with one or more runs)
3	Moderate leakage at M.T. and/or N.R. to nozzle interfaces (with appreciable boron deposits adherent to the flange)
4	Heavy leakage with boron bridging adjacent flange surfaces
5	Excessive boron accumulations on the insulation below the nozzle

In 1990 (6RFO), gaskets were replaced in 23 CRDM flanges. Figure 28 shows the leaking flanges. There are no specific records indicating an inspection of the RPV head.

In 1991 (7RFO), the RCS engineer reported an excessive amount of boron on the RPV head. The boron flowed through the mouse holes and stopped on the RPV head flange by the closure bolts. The CRDM flanges were inspected and 21 were identified as leaking and 15 were repaired. Figure 28 shows all the leaking flanges identified in 1991 and the flanges that were justified for use-as-is.

In 1993 (8RFO), an inspection of the RPV head was performed, shown in Figures 29-32. In Figure 29, the boron deposits are dripping through the gaps in the insulation forming stalactites. The boron deposits started forming stalagmites on the RPV head. Figures 30 and 31 show more boron deposits coming through gaps in the insulation and clinging to the side of the CRDM nozzles. The boron deposits in Figure 31 were reddish brown in color. The boron deposits on the RPV head in Figure 32 do not exhibit a clear picture of the source of leakage (i.e., CRDM flange or nozzle leakage).

Based on the results of the head inspection, the RPV head and flange was cleaned with deionized water. The effectiveness of the cleaning could not be verified in that the RPV head had already been returned to the RPV. A cleaning effectiveness inspection was recommended as a follow-up activity for the next outage. The CRDM flange inspection revealed 15 leaking flanges as shown in Figure 28. Framatome generated a non-conformance report (NCR) that noted degradation to the flange sealing surface found during the repair of CRDM nozzle 31. The corrective action taken was to perform flange surface polishing and gasket replacement. The 1993 NCR also recommended that the flange surface be machined if further leakage occurs.

In 1994 (9RFO), the CRDM flanges were inspected; however, no records have been identified indicating a visual inspection of the RPV head was completed. Performing a video inspection of weep holes was an activity in the outage schedule. There were no boric acid deposits interference problems with inspection equipment reported. Eight CRDM flanges were identified as leaking and repaired during this outage (Figure 28).

### **10RFO (1996)**

Figure 20 provides an overview of the boric acid deposits on the RPV head from 10RFO to 13RFO.

In 10RFO, the remaining ten flanges without the new gasket material were upgraded. As discussed in PCAQR 98-0649, and as confirmed in interviews with the engineer responsible for performing inspections of the CRDM flanges during 10RFO, one CRDM exhibited signs of minor leakage in 10RFO. The 10RFO's head visual inspection under the insulation, the majority of the RPV head was inspected except for the top center. A couple of nozzles are shown in a couple of background frames (Figures 33 and 34). These frames are approximately two to three nozzles away from the top center of the RPV head. The most conservative assumption that can be made from these figures is that boric acid extended from behind nozzles 2, 3, 4, and 5 to the bottom of the insulation. The assumed footprint of the boric acid is shown in Figure 20. Comparing Figure 33 and Figures 29 and 30, the underside of the insulation in 1996 does not show crusted boron deposits or stalactites hanging.

The boric acid was powdery and white. Boric acid seemed to be flowing toward the mouse holes. The boric acid was very thin at the front edge with powder and small clumps of boric acid on top. Because the mouse hole locations were not periodically noted during the visual inspection, the location of this flow path is uncertain. However, based on future evidence, it is assumed to be the southeast quadrant of the RPV head. The remaining area of the RPV head was clean with speckles of white boric acid deposit. Figure 35 show a typical photo of the condition of the RPV head during this inspection. Additionally, PCAQR 96-0551 reported that there was some rust or brown-stained boron in the area around nozzle 67.

### **11RFO (1998)**

Nozzle 31 was identified as having a minor flange leak using the following criteria: 1) there were no stalactites hanging from the flange, 2) there was no boric acid bridging to adjacent flanges, and 3) there was no rust present on either the flange or the split nut rings. Initial and follow-up review of the leaking flange by Davis-Besse Plant Engineering indicated that no immediate repair was required, and that this drive should be inspected during 12RFO and repairs made as required. Framatome reiterated the recommendation from 8RFO to machine the surface of the nozzle 31 flange if further leakage occurred. Unidentified leakage data was reviewed for the past several cycles. With the numerous flange leaks present in both 7RFO and 8RFO, the highest unidentified leakage was approximately 0.3 gpm in cycle 7 and 0.4 gpm in cycle 8. The unidentified leakage in cycle 11 averaged 0.05 gpm. No Technical Specifications were exceeded even when the highest flange leakage was present. During the visual inspection of the control rod drive flanges, no interferences from boric acid accumulation on top of the insulation were identified.

During 11RFO, boric acid deposits were identified flowing out of the mouse holes in the southeast quadrant of the RPV head flange. The boric acid was a reddish rusty color. The RPV flange was decontaminated prior to the inspection of the RPV head.

The Service Water System Engineer conducted the RPV head visual inspection during 11RFO. The engineer worked with a Framatome crew using a pole-mounted camera to inspect the RPV head for "cracks in nozzles and degradation adjacent to the nozzle".

During the head visual inspection, the center nozzles were again very difficult to inspect through the mouse holes using available techniques. The engineer noted white streaks on the nozzles;

however, there was no boron hanging from the insulation. The engineer noted in a recent interview that some of the nozzles had indications of upward travel of the droplets as opposed to what would be expected (downward travel). The upward travel of the droplets was noted on several nozzles and attributed to ventilation flow. Boric acid was present in fist-sized clumps behind nozzles 9 and 13. Boric acid was collecting on the RPV head as shown in Figure 37. Boric acid seemed to be falling from the top of the RPV head and collecting behind peripheral nozzles especially in the northwest and southeast quadrants. During this outage inspection, the boric acid was noted to be a mix of white and red deposits. Upon identification of red, rusty boric acid mixed in with white boric acid on the RPV head, the engineer worked with the Framatome crew to vacuum the RPV head and remove as much boron as possible. The equipment available to do the work and the limited access to the very top of the RPV head limited the removal process. During the removal of boric acid from the RPV head, the boric acid was noted to be brittle and porous. Other than these areas of accumulated boric acid, the RPV head was basically clean. Due to the limited inspection capability, the video evidence suggests that the most conservative estimate of the boric acid present would be to assume that behind nozzles 6, 7, 8, and 9 the boric acid extends to the bottom of the insulation and tapers off to the back of the next nozzle location. The approximate footprint of boric acid on the RPV head is shown in Figure 20.

### **12RFO (2000)**

During the CRDM flange inspection, the upper camera was not positioned properly at four locations. The interference was attributed to a pile of boron on top of the insulation. The boron was a red, rusty color and hard. Normally, boron found on top of the insulation is a loose powder and in the color range from white to yellow depending upon age (based on video and interviews). The boron pile encountered during this inspection was hard and could not easily be pushed to the side with the Framatome inspection tool. The underside of nozzle 3 was caked with red boric acid deposits. The inspection of the flange interface was accomplished by lifting the lower camera to see the upper flange interface. The interference locations, as shown in Figure 39, were identified in the center of the following nozzle blocks:

- Nozzles 6, 15, 11, and 3
- Nozzles 11, 27, 32, and 16
- Nozzles 15, 31, 27, and 11
- Nozzles 1, 3, 7, and 4

Based on the CRDM flange inspection, nozzles 3, 6, 11, 31 and 51 flange leaks were repaired. The CRDM flange on nozzle 31 was machined to remove a steam cut from the seating surface.

The Service Water System Engineer that conducted the RPV head visual inspection in the previous refueling outage requested to inspect the RPV head during this outage. To prepare for the inspection, he interviewed design and mechanical engineers familiar with this component and the industry issues associated with it. Another contributing factor for the Service Water engineer to request to assist in the inspection of the RPV head was the fact that the RCS engineer was new to the Davis-Besse power plant. By assisting in the inspection, any changing conditions of the boric acid on the RPV head could be easily identified based on his experience in the 1998 inspection.

As shown in Figure 36, boric acid had accumulated on the RPV head flange behind the studs flowing out of the mouse holes in the southeast quadrant. The boric acid still had a red, rusty appearance. The mouse holes in this quadrant were significantly blocked with boric acid

deposits. With the studs in place on the RPV head flange and the accumulation of boric acid, the inspection through the mouse holes was significantly hampered. The engineer requested that the RPV flange be decontaminated and the studs removed to afford a better inspection. This work was completed. Boric acid on the RPV head was identified as an outage issue.

The RCS engineer supervised the cleaning effort, which entailed the following:

- Pressurized (approximately 200 psi), demineralized water heated to 175°F.
- Water was sprayed on the boron deposits through the mouse holes and ventilation duct openings.
- Estimated volume of water 100 to 600 gallons.
- An inspection video was required post cleaning.
- If the video revealed boric acid remaining on the RPV head, the cleaning steps were expected to be repeated.

The RCS engineer acknowledges that the cleaning was not 100% successful and some boric acid deposits were left behind on the RPV head. The engineer stated that he was running out of time to continue cleaning the RPV head (the RPV head was scheduled to return to the RPV during the next shift). Outage management concurred that no additional time and dose should be spent because further attempts would not produce successful results and the results were believed to be acceptable. Radiation Work Permit (RWP) 2000-5132 package was written as a tool to control radiological exposure for cleaning boric acid from the RPV head on April 6, 2000. The RWP identified 30 man-hours and a 100 mRem dose was estimated for the work. There were 282.31 man-hours and 1611 mRem expended for cleaning the RPV head.

No written evaluation was performed to allow the boric acid to remain on the RPV head. At this point in time, the modification to cut the openings in the service structure was scheduled for the next outage. With these openings and a more aggressive cleaning technique, the RPV head could be completely cleaned of the boric acid deposits and inspected. The amount of boric acid deposits left on the RPV head can not be estimated.

#### **13RFO (2002)**

During the CRDM flange inspection, the camera again encountered a boron pile in the vicinity of nozzle 3 making the inspection of the underside of the flange difficult. No flange leakage was identified during this outage indicating that previous repairs were successful.

The engineers responsible for inspecting the CRDM flanges reported boric acid deposits flowing out of the mouse holes and piled up to 4 inches high in the southeast quadrant on the RPV head flange and extending 360° around the RPV head flange. The boric acid deposits in the southeast quadrant were hard-baked, whereas the deposits around the remainder of the RPV head flange were loose. During the inspection of the RPV head under the insulation, significant boric acid was encountered in the southeast quadrant. In the remaining quadrants, significant piles of boric acid were encountered two to three nozzles in towards the center of the RPV head as shown in Figure 24. The deposits were hard, porous deposits and were a mixture of reddish brown and white deposits. The deposits were removed by hydrolasing, which operates at approximately 2,000 psi.

Documentation Available for Review

	RPV Head Flange	RPV Head Under Insulation	Accumulation Above Insulation
Prior to 1996	PCAQR 91-0353	Video	
10RFO (1996)		PCAQR 96-0551 Video	
11RFO (1998)	Pictures	PCAQR 98-0767 & 98-0649 Video	
12RFO(2000)	CR 2000-0782 Pictures	CR 2000-1037 Video	CRDM Flange Inspection Video
13RFO (2002)	CR 2002-00685 Video	CR 2002-00846 Video	CRDM Flange Inspection Video

PCAQR: Potential Condition Adverse to Quality Report

CR: Condition Report

### 3.3.4 Containment Air Cooler Cleaning

The CAC system is an engineered safety feature and is provided, in conjunction with the Containment Spray System, to meet the requirements of 10 CFR 50, Appendix A, General Design Criteria (GDC) 38, Containment Heat Removal. It consists of three separate tube/fin fan-coolers, one associated with each of two trains. Two of the three coolers are associated with each of two safety related trains. The third cooler is a swing cooler (spare) and can be aligned mechanically and electrically to take the place of either of the other two coolers. Service water, ultimately supplied from Lake Erie, is supplied directly through the cooling coils to remove heat from Containment under both normal operating or accident conditions. The system has safety functions to cool CTMT during postulated accident conditions such as Loss of Coolant Accidents and Steam Line Breaks. During postulated accidents, operating in slow speed, each CAC is designed to move 58,000 cfm. During normal operation, the CACs are operated in high-speed and are available to remove normal process heat in CTMT, maintaining a maximum air temperature of 120°F at the inlet of the CACs. The three CACs are located in a row, next to each other, on the 585' elevation in CTMT. All CAC inlet air is drawn in at this location through the sides of the tube banks by the fan. The cooled discharge air supplies a distribution network inside the secondary shield structures, the reactor incore instrument tank, and RPV regions. The outside surfaces of the tube banks are readily visible from outside the coolers.

During operation, the service water supplied to the CACs is typically between approximately 40°F and 75°F. Being substantially cooler than CTMT, depending on CTMT humidity, the CACs remove water from the CTMT by condensation on the fin surfaces. This action would be expected to vary throughout the year. Both the dampness of the fin surfaces and high volumetric air flow rate cause the CACs to readily acquire a loading of boric acid particulate material, if it is present. In addition to collecting on the CAC cooling fins, boric acid accumulations have been observed and removed from CAC ductwork. For example, approximately 75 gallons (10 cubic feet) of wet boric acid were removed from the CAC plenum during 13RFO. Fouling of the CACs can be trended remotely by indication of plenum pressure. At Davis-Besse a fouling



condition occurred in 1992 (PCAQR 92-00072) due to a leaking flange on the primary side of a steam generator. Inspection of the CACs at that time revealed that the CACs were evenly fouled with white boric acid, which was readily cleaned with either steam or hot water sprays. After repair of the flange leak, the fouling of the CACs ended and no further cleanings (for rapid boric acid fouling) were needed for several years.

In October of 1998, there was a concern over the configuration of the pressurizer code safety valve discharge piping configuration. In brief, the safety valves discharged to a piping tee, with a rupture disc on each branch. Any weeping from the safety valves would be contained by the rupture discs and conducted to the pressurizer quench tank through a small drain line, quantified, and not counted as unidentified leakage. The tee was used with the design assumption that both rupture discs would simultaneously relieve if the code safety valves actuated. This would produce equal and opposite piping reactions, canceling each other to produce a zero net bending moment. After it was postulated that one or the other, but not both discs might relieve, it was realized that the design could result in a very large moment. Short term remedial action to resolve that concern involved deliberately failing the rupture disks. In November of 1998, PCAQR 98-1980 identified that fouling of the CACs appeared to be resuming, based on plenum pressure trends, coinciding with increased leakage from the pressurizer safety valves. Cleaning of the CACs continued, with 17 cleanings being needed between November 1998 and May 1999. During the May 1999 mid-cycle outage, a pressurizer code safety valve piping modification resolved that issue. However, two subsequent CAC cleanings were still required, one in June 1999 and another in July 1999. Although the boric acid was generally reported to be white, a written post-job critique was located from the July 1999 cleaning that indicated a "rust color" was noticed "on and in the boron being cleaned away" from CAC 1.

After 12RFO, in June 2000, CAC plenum pressure again began to decrease (CR 2000-1547), requiring resumption of cleaning. This was followed by five total cleanings in June, August, October and December of 2000. Cleanings continued in 2001, with four more (total) in January, February, March, and May. Following May 2001, the need to clean the CACs ended for the balance of the operating cycle.

During 12RFO, some CRDM flange leakage was repaired. Following 12RFO, but before 13RFO, it was not known whether those repairs had been fully successful. Therefore, the CAC cleaning could potentially have been attributed to CRDM flange leakage. However, 13RFO inspections revealed that the CRDM flange repairs in 12RFO were apparently successful. Further, earlier experience with leaking flanges (pre-1992, and 1993 – 1998) did not result in the need to clean CACs. Therefore, CRDM flange leakage can now reasonably be ruled out as the cause of the cleaning of the CACs after 12RFO.

Attributing the need for CAC cleaning to leaking CRDM nozzles is plausible, but has several inconsistencies that would need to be explained. The most prominent is that if nozzle leakage continued on an increasing trend from May 2001 until February 2002, why did the need to clean CACs end in May 2001? The answer to this question can only be postulated and will not be known unless a different source of leakage is later identified. However, there are several potential explanations. These are related to CTMT humidity vs. SW temperature over the period, to reduction in RCS boron concentration at the end of the fuel cycle, but also possibly to changes in the morphology of the nozzle leak. For example, if the corrosion cavity at CRDM nozzle 3 enlarged substantially during the last half of the fuel cycle (affecting exit velocity), or the boric acid cap contained the leakage differently, the nature and amount of particulate matter might have changed. Larger particles might settle and not be subject to ingestion by the CACs. (The

later theory has some anecdotal support based on observations that the boric acid dust on horizontal CTMT surfaces was more granular in 13RFO, as opposed to fine powder in earlier outages). However, this conjecture is subject to the similar pitfalls of the earlier (disproved) hypothesis that CRDM flange leakage (circa 1999) was different from CRDM flange leakage (pre-1992) and was therefore able to cause CAC fouling.

In summary, there was circumstantial evidence that CAC fouling was related to nozzle leakage prior to 13RFO. Because of variations in plant conditions, CAC fouling, by itself, could not be directly correlated with CRDM nozzle leakage.

### **3.3.5 Containment Radiation Monitor RE4597 Observations & Filter Plugging**

Radiation monitors RE 4597AA and RE 4597BA are two identical CTMT air sample monitoring systems, each with three detection channels and two sample locations. The monitors provide two of the three RCS leakage detection methods described by Reg. Guide 1.45 and required by TS 3.3.3.1 and 3.4.6.1, namely CTMT particulate and noble gas activity detection. These parameters are monitored because of their sensitivity and rapid response to leaks in the Reactor Coolant Pressure Boundary. Detection of radioactive iodine is also provided. A continuous sample drawn from CTMT passes through a fixed particulate filter, an iodine cartridge, and a pump. The sample then passes through a noble gas chamber and is discharged back to containment atmosphere. The containment radioactive gas monitor is less sensitive than the containment air particulate monitor and would function in the event that significant RC gaseous activity existed from fuel cladding defects. The normal sample location of RE4597AA is approximately 4 feet above the top elevation of the South wall of the West secondary shield structure in CTMT (see Figure 40). The alternate sample location is below the polar crane, at approximately 270 degrees azimuth (due West) in CTMT. The normal sample location of RE4597BA is approximately 4 feet above the top elevation of the East secondary shield structure in CTMT, but against the CTMT wall at approximately 90 degrees azimuth (due East). The alternate sample location is by the stairway to the incore instrument tank platform on the 603' elevation (i.e., near the personnel lock).

The areas of interest pertaining to the Containment Radiation Monitors revolves around two issues: 1) their capability to detect a leaking CRDM nozzle directly by their output indication, or 2) other incidental maintenance observations. For the case in point, the maintenance observations centered on unusual collection of boric acid and iron deposits on the filter elements of the monitors, necessitating frequent replacement. These points are discussed in the following paragraphs.

#### **Particulate Monitor (Channel 2)**

The containment airborne particulate monitor measures the buildup of particulates on a fixed filter and compares this to the integrated sample flow that produced the particulate buildup. In five minutes the airborne particulate radioactivity monitor can detect the increase in particulate radioactivity concentrations from a 0.1 gpm reactor coolant leak into the containment vessel postulated to occur when reactor coolant fission product activity concentrations result from 0.1% failed fuel at the beginning of core life (4 EFPD). Once in the equilibrium cycle with 0.1% failed fuel, a 1 gpm leak can also be detected in five minutes. The particulate monitor consists of a fixed particulate filter in a 3 inch 4 pi lead shield. A beta detector is inserted into the lead shield to detect the activity deposited on the filter paper. The filter paper is 99 percent efficient for 0.3 micron and larger particles. The output from the detector is fed to the microprocessor where the counts per minute are converted to  $\mu\text{Ci/cc}$ . Although this detector is effective in identification of